Optimal Fishery with Coastal Catch

Dieter Grass*, Hannes Uecker†, Thorsten Upmann‡

January 9, 2019

Abstract

In many spatial resource models it is assumed that an agent is able to harvest the resource over the complete spatial domain. However, agents frequently only have access to a resource at particular locations at which a moving biomass, such as fish or game, may be caught or hunted. Here we analyze an infinite time horizon optimal control problem with boundary harvesting and (systems of) parabolic PDEs as state dynamics. We formally derive the associated canonical system, consisting of a forward–backward diffusion system with boundary controls, and numerically compute the canonical steady states and the optimal time dependent paths, and their dependence on parameters. We start with some one–species fishing models, and then extend the analysis to a predator–prey model of Lotka–Volterra type. The models are rather generic, and our methods are quite general, and thus should be applicable to large classes of structurally similar bio–economic problems with boundary controls.

Keywords: optimal boundary control; bioeconomics; infinite time horizon; Pontryagin's Maximum Principle; optimal harvesting; bistable model; predator–prey model

Contents

*ORCHOS, Institute of Statistics and Mathematical Methods in Economics, Vienna University of Technology, A-1040 Vienna, Austria, dieter.grass@tuwien.ac.at

†Institut für Mathematik, Universität Oldenburg, 26111 Oldenburg, Germany, hannes.uecker@uol.de

‡Helmholtz-Institute for Functional Marine Biodiversity at Oldenburg University (HIFMB), 23129 Oldenburg, Germany; Bielefeld University, Faculty of Business Administration and Economics, Germany; CESifo, München, Germany; thorsten.upmann@hifmb.de

1 Introduction

Optimal control (OC) theory is an important tool to design optimal harvesting strategies in the management of natural resources. Much of the literature considers only the temporal dimension, see, e. g., the monographs Conrad et al. 1987; Conrad 2010 and Clark 2010, but recent work captures the spatial dimension as well. Early spatial models feature discrete patches, where at each location of the resource the stock evolves according to an ordinary differential equation (ODE). Migration of the biomass is then modeled as entry and exit of the biomass from one location to the other, see, e.g., Sanchirico et al. 1999; Behringer et al. 2014, and the references therein. However, in many cases the continuous process of migration is more adequately described by partial differential equations (PDEs) characterizing the spread or diffusion of the resource within the domain.

For the case of ODE–constrained optimal control problems, a main tool is Pontryagin's Maximum Principle providing first order necessary optimality conditions (Pontryagin et al. 1962), see also Aniţa 2000; Lenhart et al. 2007; Grass et al. 2008; Aniţa et al. 2011 for textbook expositions, including many examples related to natural ressources. In bioeconomics, the objective often contains a discounted time integral

$$J = \int_0^T \mathrm{e}^{-\rho t} J_c(v(t), u(t))\,\mathrm{d}t, \tag{1}$$

where $\rho > 0$ is a discount rate, $v(t) \in \mathbb{R}^n$ are the states of the system, $u(t) \in U \subset \mathbb{R}^p$ represents the controls, and J_c is called the current value function. If $T = \infty$ in (1), then we have an *infinite time horizons*, while for $T < \infty$ we have a *finite time horizon.* Also for PDE–constrained optimal control problems a large theory has been developed, see, e.g., Lions 1971; Li et al. 1995; Hinze et al. 2009; Tröltzsch 2010. Some maximum principles have been rigorously established in an abstract way, assuming a priori the existence of optimal solutions, but almost exclusively for the finite time horizon case. See §3 for further comments and references.

In a number of bio-economic and resource–economic papers, e.g., Fister 1997; Lenhart et al. 1999; Fister et al. 2006; Ding et al. 2009; Kelly et al. 2016; Baker et al. 2018, the

existence of optimal controls, and subsequently the validity of the Pontryagin's Maximum Principle, has been proven on a case by case basis using some minimizing sequence and compactness arguments, see also Lenhart et al. 2007, Chapter 25 and Aniţa et al. 2011, Chapter 5. However, all these works consider steady problems or finite time horizons. More specifically, Fister 1997 considers spatially distributed harvesting of both the prey and the predator (on the full spatial domain) in a predator–prey diffusive model population. In Fister 2001, the economic agent is interested in harvesting the predator only, but the model also introduces a boundary control which allows for controlling the migration of the populations across the boundary (e. g., a fence, mesh size of a net, filter). Similarly, the further works refered to above consider OC in a bio-economic time dependent diffusive setting. One common result of these works is that for distributed harvesting it may be (economically) advantageous to have zones of no or substantially reduced harvest ('marine reserves' in the context of fisheries). The population may then grow to a high level in the no–harvest zone, and the 'spillover' by diffusion gives a higher yield than the one obtained from a uniform harvesting. See also Leung 1995; Neubert 2003 for similar results for steady state problems.

For the PDE case with infinite time horizons, Pontryagin type optimality conditions have been proven for some linear PDE problems with linear–quadratic objectives, e.g., Barucci et al. 2001; Faggian 2004; Faggian et al. 2013; Boucekkine et al. 2013; Ballestra 2016. For genuinely nonlinear problems with diffusion such conditions have been formally derived in Brock et al. 2008. See also Xepapadeas 2010; Brock et al. 2010; Uecker 2016; Grass et al. 2017 for applications that in particular may lead to the emergence of spatial heterogeneity of the resource and the harvesting.

Here we assume an infinite time horizon and a spatially distributed resource for which harvesting can only be done on the boundary of the spatial domain. This constraint may result from legal or physical restraints where the agent is not allowed or not able to harvest inside the habitat. For instance, often a substantial part of fishing is done at the shore or near the shore by artisanal fisheries; also, since fishing or hunting may be banned within protected areas, such as nature reserves, marine protected areas, game reserves etc., fishing and hunting frequently happens at the boundaries of those protected areas, aiming at the spillover to the non–protected areas (Fogarty et al. 2004; Kellner et al. 2007; McCauley et al. 2016). Moreover, harvesting may be further restricted to subsets of the boundary, e.g., to certain places at the shore of a lake. Specifically, we consider classes of infinite time horizon optimal control fishery problems with diffusion, boundary catch, and classical Cobb–Douglas production functions. We start with some one-species problems, and then extend the analysis to a two-species predator–prey model. We formally (i.e., a priori assuming the existence of optimal controls, see §3.3 for further comments) derive the so called canonical systems, i. e., necessary first order optimality conditions. The associated stationary problems are systems of non-linear elliptic PDEs,

which, depending on the parameter regimes, may have multiple solutions, and in order to first obtain a comprehensive picture of these so called canonical steady states we use the continuation and bifurcation software `pde2path` (Uecker et al. 2014). In a second step, we compute canonical paths to canonical steady states and compare their values, and thus characterize policies to reach optimal steady states in a profit-maximizing way.

It turns out that for both classes of models, i. e., the scalar one and the interacting species model, generally speaking a "moderate harvesting policy" is optimal. This is quite intuitive as excessive fishing leads to a drastic diminution of the stock and thus impairs the conditions for future yield. A moderate fishing activity forgoes present profits, but saves some of the stock for later growth and catch. However, some results of our analysis are quite intriguing already for one of our scalar models, distinguished by a bistable growth function. Here, the space of initial states is divided into three sets, namely 'sub-threshold' initial states from which we can only reach low–stock canonical steady states, 'super-threshold' initial states from which we can only reach high–stock canonical steady states, and a rather small 'intermediate' set from which we can reach both.

We complement our analysis by discussing the spatial distributions of the respective co-states or shadow prices. While in the one-species models the shadow price of fish is falling with the distance from the shore, this does not necessarily hold for the predator in the two-species case, even though the net market value of the predator species is positive. Moreover, the asymmetric interaction between both species gives asymmetric cost effects: While an increase in the fishing cost of the prey results in an increase in both stocks, an increase in the fishing cost of the predator leads to a decrease in the stock of the prey. In particular, if fishing of the predator is relatively costly, its value may become negative, even though its market price exceeds the harvesting cost. Of course, here we leave the gap that we apply the Pontryagin's Maximum Principle in a formal way. Still, we identify candidates for optimal solutions, and we believe that our analysis makes a methodological contribution beyond the specific insights into optimal boundary fishing: our approach can be applied to other PDE problems with controls restricted to the boundary of the domain, and is rather independent of the functional forms of the state PDEs and the objective function.

To the best of our knowledge, such infinite time horizon boundary harvesting problems have not yet been considered in the bio-economic literature. Fister 2001 considers a finite time horizon problem, and, additionally to distributed controls, a rather special boundary control which is not directly connected to harvesting. Kellner et al. 2007 focuses on steady states, and the boundary harvest is not strictly at the boundary. Moreover, both use simple quadratic expressions for the yields as functions of efforts and stocks.

The remainder of the paper is organised as follows. In §2 we describe our models, and also provide a phase plane analysis of the constraints for the scalar stationary case. In §3 we formally derive the canonical system for the scalar case, discuss this formal derivation,

and describe the basic numerical method for their solution. In §4 we present the results for the one species models. Results of the two-species model are in §5, and in §6 we conclude by discussing possible extensions and future research directions.

2 Problem setup

2.1 A class of scalar models

Consider a fishery problem where harvesting (fishing) can be done on the boundary of some area, for example, a fisher catching fish from the shore. For simplicity we consider a one-dimensional space represented by the interval $\Omega := (0, l)$, with fishing only at location $x = 0$, the position of the fisher. Let $v = v(x, t)$ be the biomass of fish at location $x \in \Omega$ at time $t \geq 0$. The catch depends on the available biomass of fish v and on the harvesting effort k of the fisher, who wants to maximize his profit. We specify the catch (or harvest) as a standard Cobb–Douglas function,

$$h = h(v, k) = v^{\alpha} k^{1-\alpha} \tag{2}$$

with $0 < \alpha < 1$. Let $p > 0$ denote the market price of one unit of fish, and $c > 0$ the (constant) per unit cost of harvesting effort. Since fish is a non-durable good, the catch is offered at the market immediately when it is realized. Thus, we model the instantaneous profit from harvesting as

$$J_c(v, k) = ph(v, k) - ck. \tag{3}$$

The evolution of the stock is governed by net growth of the biomass and movement of fish. Possible growth functions are

$$f(v) = f_{\text{lin}}(v) := \delta - \beta v \qquad \text{(linear)}, \tag{4a}$$

$$f(v) = f_{\text{log}}(v) := v(\delta - \beta v) \qquad \text{(logistic)}, \tag{4b}$$

$$f(v) = f_{\text{bi}}(v) := -(v - \delta)(v - \beta)(v - 1) \qquad \text{(bistable)}, \tag{4c}$$

with parameters $\delta, \beta > 0$, respectively $0 \leq \delta < \beta < 1$ for f_{bi}. For $f = f_{\text{lin}}$, the ODE $\dot{v} = f(v)$ has the unique globally stable fixed point $v^* = \delta/\beta$. For $f = f_{\text{log}}$ we again have the stable fixed point v^* and, in addition, the unstable fixed point $v = 0$. For our purposes both models are quite similar: In particular, for each set of parameters both have a unique *canonical steady state* (CSS) (which refers to steady states of the canonical system (CS), see below), showing similar qualitative behavior. The main difference is that for f_{lin} we can compute these CSSs semi-analytically, see §4.1.1, which can also be used to validate the numerics.

For f_{bi} we have the stable fixed points $v{=}\delta$ and $v{=}1$, and the unstable fixed point $v{=}\beta$. For $\delta{=}0$, f_{bi} models critical depensation, see, e.g., Conrad et al. 1987, p. 63, Da Lara

et al. 2008, p. 18f, here meaning that in order to grow the stock needs to be beyond the threshold β, e.g., for mating reasons (Allee effect). The parameter $\delta > 0$ could be used to describe some small constant external input, i.e., $f_{\mathrm{bi}}(0) = \delta\beta > 0$, but we rather see δ as a regularization parameter, because h in (2) is not differentiable at $v = 0$ or $k = 0$, i.e., $\lim_{v\to 0} \partial_v h(v, k_0) = \lim_{k\to 0} \partial_k h(v_0, k) = \infty$ for all $v_0, k_0 > 0$. In economics, this models infinite marginal values (Inada conditions) at low stocks/harvesting efforts. For (initially) large stocks we can also work with $\delta = 0$, but here we shall also be interested in the case of optimal harvesting of low initial stocks. For $\delta > 0$ we can derive and solve the CS, and obtain well behaved (steady and time dependent) solutions with low v. We can then a posteriori take the limit $\delta\to 0$ which yields a well defined limit CS. Moreover, the (steady and time dependent) solutions of the CS for $\delta>0$ converge to solutions of the limit CS, and although we do not have a rigorous proof this strongly suggests that the (low stock) solutions of the limit CS yield optimal solutions of the problem with $\delta=0$. Altogether we find that $f=f_{\mathrm{bi}}$ gives a much richer problem than f_{lin} and f_{log} do.

The movement of fish is modeled as diffusion, i. e., by a term proportional to Δv, where Δ denotes the Laplace operator with respect to x.[1] Thus, the biomass of fish evolves according to the system of differential equations and boundary conditions (BC)

$$\partial_t v = -G_1(v) := D\Delta v + f(v) \quad \text{in } \Omega \times \mathcal{T}, \tag{5a}$$

$$\partial_n v(l, t) = 0 \quad \text{in } \mathcal{T} \text{ (zero flux at the right boundary)}, \tag{5b}$$

$$D\partial_n v(0, t)+g(v(0, t), k(t))=0 \quad \text{in } \mathcal{T} \text{ (control-dependent flux at the left boundary)}, \tag{5c}$$

$$v(x, 0) = v_0(x) \quad \text{in } \Omega, \tag{5d}$$

where D is the diffusion coefficient, n denotes the exterior normal to the boundary $\partial\Omega$. In the one-dimensional case we could assume (by rescaling the domain) that $D = 1$, but for conceptual clarity and generalizations we keep D. The zero-flux (or Neumann) boundary condition at $x = l$ model that no fish can leave or enter. The harvesting at the left boundary of Ω gives the flux boundary condition (5c): if $g > 0$, then also $\partial_x v(0, t) = -\partial_n v(0, t) = \frac{1}{D} g > 0$, meaning that $x \mapsto v(x, t)$ is an increasing function. Since g is induced by the harvest h, we set

$$g(v, k) = \gamma h(v, k), \tag{5e}$$

for some $\gamma > 0$. Hence, a larger take out of fish at $x = 0$ increases the differential in stocks between $x = 0$ and its (right) neighborhood $x > 0$, and γ can be thought of as the inverse of the replacement flux of fish: when γ is high (low) a given amount of fishing leads to a large (small) differential in stocks near $x = 0$, and this differential is due to a slow (fast) replacement of fish due to diffusion. Thus, in a simple setting γ could be

[1] Although we focus on the one dimensional case $\Omega = (0, l)$, where $\Delta v = \partial_x^2 v$, we use dimension-independent notation where suitable for the purpose of possible generalization. Note that $\partial_n v(0, t) = -\partial_x v(0, t)$ and $\partial_n v(l, t) = \partial_x v(l, t)$.

chosen proportional to $1/D$, but we keep it as an independent parameter, essentially to possibly model special conditions for the replacement fluxes at the boundary.

Finally, given the instantaneous profit J_c from (3), the fisher seeks to maximize the total discounted profits

$$V(v_0) = \max_{k \in C([0,\infty),\mathbb{R}^+)} J(v_0, k), \text{ where } J(v_0, k) := \int_0^\infty \mathrm{e}^{-\rho t} J_c(v(0,t), k(t))\,\mathrm{d}t. \tag{5f}$$

We thus have an optimal control (OC) problem with the PDE constraints (5a)–(5e) and the boundary control $k : [0,\infty) \to [0,\infty)$. In particular, we do not impose an upper limit on the harvesting effort k. Instead, it turns out that k is bounded above, and that the natural constraint $k \geq 0$ is automatically fulfilled, i.e., never becomes active.

2.2 Phase plane analysis of the steady state constraint

To get an intuition for the constraints in (5), we first sketch a phase plane analysis of the constraint in the stationary case, i. e., for the scalar ODE

$$Dv'' + f(v) = 0, \tag{6}$$

where as a shorthand we write $v' \equiv \partial_x v$ and $v'' \equiv \partial_x^2 v$. Equivalently we can write (6) as a spatial dynamics system

$$v_1' = v_2, \quad Dv_2' = -f(v_1), \tag{7}$$

which is Hamiltonian with conserved energy $E(v, v') = \frac{1}{2}Dv'^2 + F(v)$, with $F' = f$, because $\frac{\mathrm{d}}{\mathrm{d}x}E(v(x), v'(x)) = v'(x)(Dv''(x) + f(x)) = 0$, and hence the orbits are level lines of E. For the specifications of f given in (4), we obtain

$$F_{\mathrm{lin}}(v) = \delta v - \frac{\beta}{2}v^2, \quad F_{\mathrm{log}} = \frac{\delta}{2}v^2 - \frac{\beta}{3}v^3, \tag{8}$$

$$F_{\mathrm{bi}}(v) = \delta\beta v - \frac{1}{2}(\beta + (1+\beta)\delta)v^2 + \frac{1}{3}(1+\beta+\delta)v^3 - \frac{1}{4}v^4. \tag{9}$$

Clearly, for all three, $(v_1, v_2) = (1, 0)$ is a saddle point of the energy. From the modeling we know that we should only be interested in orbits of (6) with $v(x) > 0$ for all $x \in (0, l)$, with $v'(l) = 0$, and with $v'(0) > 0$ because we want a positive take-out at $x = 0$. Thus, the only relevant solutions of (6) are those which start at $x = 0$ with $v(0) > 0$ and $v'(0) > 0$.

Figure 1(a,b) illustrates that f_{lin} and f_{log} behave rather similarly in the pertinent region of the phase plane, i. e., north-west of the fixed point $(1, 0)$, but f_{bi} in (c,d) is qualitatively different. The black orbit in (c) is similar to those in (a,b), i.e., it starts northeast and 'near' the fixed point $(1, 0)$. Additionally, see (d), there are now orbits (blue example) that start at low v and v' and end near $(1, 0)$, and orbits (magenta example) that start left of the low fixed point $(\delta, 0)$. Now, an immediate question is: For a given model, f_{lin}, f_{log} and f_{bi}, which of its steady states maximize J_c in the set $\mathcal{S}$ of steady

states? Moreover, we are interested in the solution of the intertemporal OC problem (5). Thus, we next *formally* derive the necessary first order optimality conditions, known as the canonical system (CS), with steady solutions called canonical steady states (CSSs). Returning to Fig. 1, for both, f_{lin} and f_{log}, at a given set of parameters there will be a unique CSS, which corresponds to one of the black orbits in (a,b), respectively. However, for $f{=}f_{\text{bi}}$ there will generically be multiple CSSs.

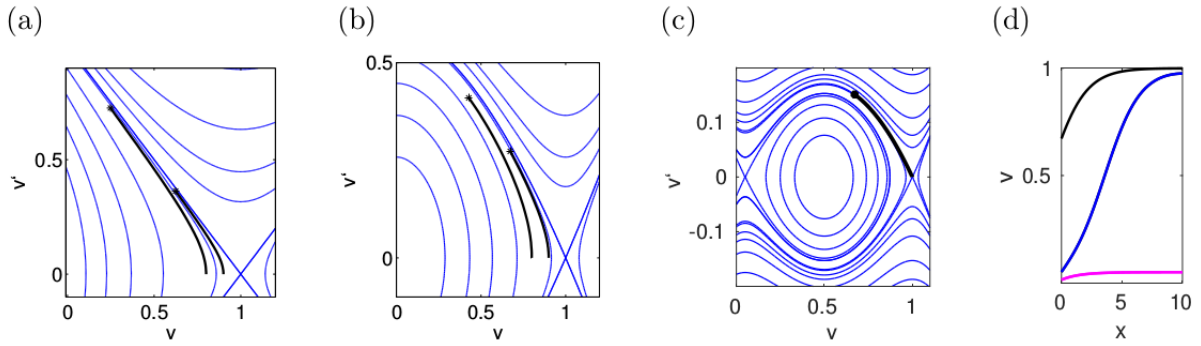

Figure 1: Phase plane analysis for (7), with (a) $f = f_{\text{lin}}$ and (b) $f = f_{\text{log}}$, both without loss of generality with $\delta = \beta = D = 1$, and (c) $f = f_{\text{bi}}$ with $\beta = 0.5, \delta = 0.05$. The blue lines are the level lines of the respective E, thus giving the phase portrait, while the black orbits (in (a,b)) are obtained from choosing $v(l)$ near 1, $v'(l) = 0$, i. e., $(v_1, v_2)(l)$ near the fixed point $(1, 0)$, and integrating "backward in time" to $x = 0$, here for illustration with $l = 2$. The black points thus indicate the "initial condition" at $x = 0$. We obtain qualitatively similar behavior for all $l > 1$, say, with the only difference that for larger l the "endpoints" of the black orbits must be closer to the fixed points in order that the solutions are in the first quadrant. In (c) we proceed similarly for f_{bi} with $l = 10$. In (d) we plot $v(t)$ for three orbits; the black orbit is from (c), while the blue one corresponds to a slightly smaller $v(l)$, and the magenta one to nearly constant v near the fixed point $(v, v') = (\delta, 0)$.

2.3 A predator–prey system

The scalar model of §2.1 can be greatly generalized. As an example, consider a standard Lotka–Volterra system for prey (v_1) and predator (v_2) in the form

$$\begin{aligned} \partial_t v_1 &= d_1 \Delta v_1 + (1 - \beta v_1 - v_2) v_1, \\ \partial_t v_2 &= d_2 \Delta v_2 + (v_1 - 1) v_2, \end{aligned} \tag{10}$$

with diffusion constants d_j, and self damping parameter of the prey $\beta > 0$. This system can more compactly be written as $\partial_t v = -G_1(v) = D\Delta v + f(v)$, with $D = \begin{pmatrix} d_1 & 0 \\ 0 & d_2 \end{pmatrix}$ and growth function $f(v) = \begin{pmatrix} (1 - \beta v_1 - v_2) v_1 \\ (v_1 - 1) v_2 \end{pmatrix}$. Using the Liapunov function $\phi(v_1, v_2) = v_1 + v_2 - \ln v_1 - (1 - \beta) \ln v_2$ it follows that

$$V^* = (v_1, v_2) = (1, 1 - \beta) \tag{11}$$

is the unique steady state of the ODE system $\frac{\mathrm{d}}{\mathrm{d}t}v = f(v)$ in the first quadrant, and is globally stable. Similarly, using the functional

$$\Phi(t) = \int_\Omega \phi(v_1(t,x), v_2(t,x))\,\mathrm{d}x \tag{12}$$

it follows that for $d_{1,2}$ sufficiently large, V^* is the unique steady state of (10) with zero flux BC, and is globally stable, see, e. g., Hastings 1978. For $v_2 \equiv 0$, the v_1 equations corresponds to the case $f = f_{\log}$ from §2.1, and we have the additional fixed point $(v_1, v_2) \equiv (1/\beta, 0)$, but here and in the following we always restrict to $v_1, v_2 > 0$.

Analogous to (5) we consider a boundary fishing problem for (10). We introduce J and fishing efforts k_1, k_2 as controls via

$$J_c = \sum_{j=1}^{2} p_j h_j - c_j k_j, \quad h_j = h_j(v_j, k_j) = v_j^{\alpha_j} k_j^{1-\alpha_j}, \tag{13}$$

$$d_j \partial_n v_j = -g_j := -\gamma_j h_j \quad \text{as left BC}, \tag{14}$$

and want to maximize

$$V(v_0) = \max_{k \in C([0,\infty), \mathbb{R}^2_+)} J(v_0, k), \text{ subject to (10) and (13), (14)}, \tag{15}$$

where $J(v_0,k) := \int_0^\infty \mathrm{e}^{-\rho t} J_c(v(0,t), k(t))\,\mathrm{d}t$, with the vector valued initial states $v_0 : \Omega \to \mathbb{R}^2_+$, and the vector valued boundary control $k = (k_1, k_2) : [0,\infty) \to \mathbb{R}^2_+$.

3 The canonical system formalism

To solve (5), and (15), we formally derive the associated canonical systems, also called state-costate or state-adjoint equations, which here take the form of forward–backward diffusion problems. We first focus on the scalar case (5), and postpone the quite analogous vector valued case (15) to §5. As already indicated in the Introduction, *formally* here inter alia means that we a priori assume that optimal controls exist. See §3.3 for further comments, and comparison with other methods and results for PDE constrained infinite time-horizon OC.

3.1 Formal derivation

We consider the Lagrangian

$$L(v, \lambda, k) := \int_0^\infty \mathrm{e}^{-\rho t} \left\{ J_c - \int_\Omega \lambda(\partial_t v + G_1(v))\,\mathrm{d}x \right\} \mathrm{d}t \tag{16}$$

where $\lambda : Q \to \mathbb{R}$, $Q := \Omega \times [0,\infty)$ is the Lagrange multiplier for the PDE constraint (5a), also called co-state variable, or, in economics, the shadow price of the biomass at

location x at time t. Using integration by parts in x we have

$$\begin{aligned}\int_\Omega \lambda D\Delta v \,\mathrm{d}x &= -\int \langle \nabla\lambda, D\nabla v\rangle \,\mathrm{d}x + \int_{\partial\Omega} \lambda D\partial_n v \,\mathrm{d}s \\ &= \int (D\Delta\lambda)v \,\mathrm{d}x + \int_{\partial\Omega} \lambda(D\partial_n v) - (D\partial_n\lambda)v \,\mathrm{d}s, \end{aligned} \tag{17}$$

and integration by parts in t yields

$$-\int_0^\infty \mathrm{e}^{-\rho t}\int_\Omega \lambda\partial_t v \,\mathrm{d}x\,\mathrm{d}t = \int_\Omega \lambda(x,0)v(x,0)\,\mathrm{d}x + \int_0^\infty \mathrm{e}^{-\rho t}\int_\Omega (\partial_t\lambda - \rho)v \,\mathrm{d}x\,\mathrm{d}t, \tag{18}$$

where we used the so-called transversality condition

$$\lim_{t\to\infty} \mathrm{e}^{-\rho t}\int_\Omega \lambda(x,t)v(x,t)\,\mathrm{d}x = 0, \tag{19}$$

which here ensures that the boundary terms at $t = \infty$ vanish. See §3.3 for further comments. Next, using the BCs (5c) and (5b), i. e., $D\partial_n v|_{x=0} = -g$ and $D\partial_n v|_{x=l} = 0$, we obtain

$$\begin{aligned} L(v,\lambda,k) = \int_\Omega v(x,0)\lambda(x,0)\,\mathrm{d}x + \int_0^\infty \mathrm{e}^{-\rho t}\Big\{ \big(J_c - \lambda g - (D\partial_n\lambda)v\big)\big|_{x=0} - (D\partial_n\lambda)v\big|_{x=l} \\ - \int_\Omega (\rho\lambda - \partial_t\lambda - D\Delta\lambda)v - \lambda f(v)\,\mathrm{d}x\Big\}\,\mathrm{d}t. \end{aligned} \tag{20}$$

The first variation of L with respect to v, applied to a test-function $\phi \in C^\infty(Q)$ with $\phi(\cdot,0) = 0$, yields

$$\begin{aligned} \partial_v L\phi = \int_0^\infty \mathrm{e}^{-\rho t}\Big\{ \big((\partial_v J_c - \lambda\partial_v g - D\partial_n\lambda)\phi\big)\big|_{x=0} - (D\partial_n\lambda)\phi\big|_{x=l} \\ - \int_\Omega (\rho\lambda - \partial_t\lambda - D\Delta\lambda - \partial_v f(v)\lambda)\phi \,\mathrm{d}x\Big\}\,\mathrm{d}t. \end{aligned}$$

Therefore, by density of $C^\infty(Q)$ in $L^2(Q)$, and by density of $\partial_n C^\infty(\Omega)$ in $L^2(\partial\Omega)$, the condition $\partial_v L\phi = 0$ yields $\rho\lambda - \partial_t\lambda - D\Delta\lambda - \partial_v f(v)\lambda = 0$ and the boundary conditions $D\partial_n\lambda|_{x=l} = 0$ and $D\partial_n\lambda - \partial_v J_c + \lambda\partial_v g = 0$. Thus, using $\partial_v J_c = p\partial_v h$ and $\partial_v g = \gamma\partial_v h$, the canonical system is

$$\partial_t v = D\Delta v + f(v), \qquad v(x,0) = v_0(x), \tag{21a}$$

$$\partial_t\lambda = \rho\lambda - D\Delta\lambda - \partial_v f(v)\lambda, \tag{21b}$$

$$D\partial_n v + \gamma h = 0 \text{ at } x = 0, \qquad \partial_n v = 0 \text{ at } x = l, \tag{21c}$$

$$D\partial_n\lambda - (p - \gamma\lambda)\partial_v h = 0 \text{ at } x = 0, \qquad \partial_n\lambda = 0 \text{ at } x = l, \tag{21d}$$

where k is obtained from $k(t) = \operatorname{argmax}_k L(v(\cdot,t),\lambda(\cdot,t),k)$. In the absence of control constraints (see the remarks after (5f)), the condition $\partial_k L = 0$ yields

$$\begin{aligned} 0 &= \partial_k J_c - \gamma\lambda\partial_k h - v\partial_k(p - \gamma\lambda)\partial_v h \\ &= p\partial_k h - c - \lambda\gamma\partial_k h - v(p - \gamma\lambda)\partial_v\partial_k h = (p - \gamma\lambda)\partial_k h - (p - \gamma\lambda)\alpha\partial_k h - c, \end{aligned}$$

and thus

$$(p-\gamma\lambda)(1-\alpha)\partial_k h = c \quad \Leftrightarrow \quad k = \widetilde{k}(\lambda)v, \quad \widetilde{k}(\lambda) = \left(\frac{(1-\alpha)^2(p-\gamma\lambda)}{c}\right)^{1/\alpha}. \tag{21e}$$

Hence, if an optimal control k for the OC problem (5) exists, then (21) gives first order optimality conditions. In particular, the optimal effort is determined by (21e), where $p-\gamma\lambda$ represents the total value of one unit of biomass. The extent to which a take out affects future catch depends on the replacement flux of fish at the boundary, measured by γ. If γ is large (small), then the replacement flux of fish is slow (fast), so that the stock recovers slowly (quickly). In economic terms, λ is the shadow price of fish, and $\gamma\lambda$ represents a future reduction of profit due to today's take out of fish, and this value must be subtracted from the market price of fish.

3.2 Numerical method

We want to solve (21) on the infinite time horizon $t \in [0,\infty)$, and thus at first might want to think of (21) as an initial value problem. However, (21a) provides initial data for only half the variables, while (21b) has backward diffusion. We proceed similar to Grass et al. 2008, Chapter 7; Uecker 2016 and Grass et al. 2017, see also Kunkel et al. 2000; Beyn et al. 2001. First, setting $u = (v,\lambda)$ we compute *canonical steady states* (CSSs) $\hat{u}$, i. e., steady states of the canonical system. Then, given some initial state v_0, we want to compute *canonical paths* (CPs) $t \mapsto u(\cdot,t) = (v(\cdot,t),\lambda(\cdot,t))$ connecting v_0 to some CSS, and from these paths the optimal control $t \mapsto k(t)$ via (21e).

Thus, write (21) as

$$\partial_t u = -G(u), \quad u := (v,\lambda), \quad u_1(x,0) = v_0(x), \tag{22}$$

where we generally suppress the dependence on parameters. The CSSs are solutions of

$$G(u) = 0. \tag{23}$$

In general, (23) is a non-linear elliptic system, and thus at a given set of parameters we may expect multiple CSSs, $\hat{u}=(\hat{v},\hat{\lambda})$, with (generically) different values $J(\hat{v})=\frac{1}{\rho}J_c(\hat{v})$, for different CSSs. If, for instance, we let 1 parameter vary in (23), then the solutions come in branches (1 dimensional continua), from which at certain parameter values new solution branches may bifurcate. To find such solution branches we use the `Matlab` continuation and bifurcation package `pde2path` (Uecker et al. 2014), designed for PDEs of type (22) (and also for more general PDEs) over one-, two- and three-dimensional domains, based on a spatial finite element method (FEM). As u in (23) always has an even number of components, in the following we write $2n$ for the spatial degrees of freedom.

A *canonical paths* (CP) connecting v_0 to some CSS $\hat{u}$ is a time dependent solution $t \mapsto u(t)$ of (22) such that

$$u_1(x,0) = v_0(x) \ \text{ and } \ \lim_{t\to\infty} u(t) = \hat{u}. \tag{24}$$

Only the first component $u_1|_{t=0}=v_0$ is fixed, while $u_2|_{t=0}=\lambda|_{t=0}$ and hence the control $k(0)$ are free. Different situations may arise:

1. There is a unique CP connecting v_0 to a CSS $\hat{u}$.
2. There is a unique CSS $\hat{u}$ which can be reached from v_0, but different CPs to do so.
3. Different CSSs $\hat{u}^{(1)}, \hat{u}^{(2)}, \dots$ can be reached from v_0, and for each target there may be more than one CP.

If, given v_0, there is more than one CP by choice of $\lambda(0)$, then we can compare the respective values of J for those paths, and decide which one is optimal. Reversely, we can also consider a given CSS $\hat{u}$ and ask from which v_0 it can be reached by a CP. In particular, a CSS $\hat{u}$ that can be reached from all nearby v_0 and such that the associated CPs maximizes $J(v_0, \cdot)$ is called a *locally stable optimal steady state* (OSS), while a CSS which can be reached from all v_0 that are admissible, i. e., here all $v_0 \geq 0$ (pointwise), and such that the CPs maximize $J(v_0, \cdot)$, is called a *globally stable* OSS. In general, all of the alternatives 1.–3. can occur in a given system. In particular, there may be multiple locally stable OSSs. See, e. g., Grass et al. 2008 for various ODE applications, and Uecker 2016; Grass et al. 2017 for some PDE examples. Additionally, there may be optimal limit cycles (Wirl 1996, Uecker 2019, §3.4), or (slow, i.e., such that (19) still holds) divergence of optimal solutions to infinity, see the AK example in §3.3.2.

To compute a CP towards a CSS $\hat{u}$, we numerically proceed as follows. Given the spatial discretization of $G(u) = 0$ with $2n$ degrees of freedom, i. e., $u = (v, \lambda) \in \mathbb{R}^{2n}$, (22) becomes a coupled system of $2n$ ODEs, which with a slight abuse of notation, we again write as

$$M\frac{\mathrm{d}}{\mathrm{d}t}u = -G(u), \quad v(0) = v_0 \in \mathbb{R}^n. \tag{25a}$$

Here $M \in \mathbb{R}^{2n\times 2n}$ is the mass matrix of the FEM. We choose a truncation time T and approximate (24) by

$$u(T) \in E_s(\hat{u}) \text{ and } \|u(T) - \hat{u}\|_\infty \text{ small}, \tag{25b}$$

where $E_s(\hat{u})$ is the stable eigenspace of $\hat{u}$ for the linearization $M\frac{\mathrm{d}}{\mathrm{d}t}\tilde{u} = -\partial_u G(\hat{u})\tilde{u}$ of (25). At $t = 0$ we already have the boundary conditions $v(0) = v_0$ for the states. Then, in order to obtain a well-defined two point boundary value problem in time we need

$$\dim E_s(\hat{u}) = n. \tag{26}$$

Since the eigenvalues of the linearization are always symmetric around $\rho/2$ (Grass et al. 2017, Appendix A) we always have $\dim E_s(\hat{u}) \leq n$. The number

$$d(\hat{u}) = n - \dim E_s(\hat{u}) \tag{27}$$

is called the *defect* of the CSS $\hat{u}$. A CSS $\hat{u}$ with $d(\hat{u}) > 0$ is called *defective*, and if $d(\hat{u}) = 0$, then $\hat{u}$ has the so called *saddle point property* (SPP). These are the only CSSs such that

for general v_0 close to $\hat{v}$ we may expect a solution for the connecting orbits problem (25a), (25b). See Grass et al. 2017 for further comments on the significance of the SPP (26) on the discrete level, and its (mesh-independent) meaning for the canonical system as a PDE. Furthermore, see Uecker 2017 for algorithmic details how to implement (25b) in `pde2path`, and how to find CPs connecting some v_0 to $\hat{u}$ by a continuation process in the initial states.

3.3 Remarks on the formal derivation and comparison with other methods

The derivation of (21) is *formal* in the sense that we assume

- that an optimal control $k : [0, \infty) \to \mathbb{R}$ exists and gives a finite value $J(k, v) < \infty$;
- that k and the associated solution $v : \Omega \times \mathbb{R} \to \mathbb{R}$ are sufficiently smooth such that the integration by parts in x and t are valid;
- that the transversality condition (19) holds.

These are non-trivial assumptions. There are simple ODE OC problems where naive application of maximum principles yields wrong results, see, e.g., Lenhart et al. 2007, Example 2.1, or Serovaiskii 2003 for various further examples and a thorough discussion.[2] Thus, it would be desirable to prove the existence of an optimal control k for (5), and to prove that (21) yields *all* candidates. However, a general theory for optimal control for PDE problem so far only exists for finite time horizons, see, e.g., Raymond et al. 1999; Casas et al. 2000; Casas et al. 2015; Casas et al. 2018. The existing general theory for infinite time horizons only deals with ODEs, and usually the existence of an optimal solution is a priori assumed. See, e.g., Grass et al. 2008, §3.7, §3.8 and the references therein, or Tauchnitz 2015.

In summary, (21) only gives *some* candidates for optimal solutions, i.e., candidates within the class for which (21) can be derived, and the solutions we obtain are necessarily regular in t and x. Thus, we cannot guarantee that there are no 'reasonable' controls k, e.g., $k \in PC^0([0, \infty), \mathbb{R}_+)$, that yield a higher J than that obtained from the candidates from (21). Moreover, we did not consider state or control constraints. However, our aim are computations for models based on the Cobb-Douglas harvesting (2) that go beyond simple models based on linear quadratic objective functionals (see §3.3.1 and §3.3.2 below). In particular, we can check *a posteriori* that all CSSs and CPs fulfill the natural constraints $k(t) > 0$ for all $t \geq 0$, and $v(x, t) \geq 0$ for all $t \geq 0$ and all $x \in \Omega$, and that both are also reasonably bounded from above. Thus, we think that the existence of controls yielding a higher objective value, not obtained via (21), is very unlikely.

[2] An even simpler example would be the function $f : \mathbb{R} \to \mathbb{R}$, $f(x) = x^3$, which has a unique solution $x = 0$ of the 'necessary conditions' $f'(x) = 3x^2 = 0$, but f has no maximum or mimimum. Also if we restrict f to $I = [-1, 1]$, then the extrema are at $x = \pm 1$ where $f'(x) = 0$ does not hold. Clearly, $f'(x) = 0$ is only necessary for inner extrema, and in any case is in general not sufficient.

On the other hand, there is some work which deals rigorously with (linear–quadratic) infinite time horizon OC problems with linear PDE constraints. In the following two subsections we give two examples and relate these to our formal analysis and the 2-step numerical approach from §3.2.

3.3.1 Age specific advertising

Faggian et al. 2013 study optimal advertising models with a linear quadratic objective, for instance of the form

$$V(v_0) = \max_{w\in\mathcal{W}} J(v_0,w), \quad J(v_0,w) = \int_0^\infty \mathrm{e}^{-\rho t}\left(\int_\Omega \pi(x)v(x,t) - \frac{\kappa(x)}{2}w^2(x,t)\,\mathrm{d}x\right)\mathrm{d}t, \quad (28)$$

subject to the first order (transport) linear PDE

$$\partial_t v = -\partial_x v - \delta v + w \ \text{ in } \ \Omega=(0,\omega), \quad v(0,t)=0, \quad v(x,0)=v_0(x). \quad (29)$$

Here, $[0,\omega]$ is an age interval of customers, $v:[0,\omega]\times[0,\infty)\to\mathbb{R}_+$ is the (age and time dependent) goodwill of the customers wrt some product, the control $w(x,t)$ is the advertising effort, distributed in age and time, and $\pi,\kappa:\Omega\to\mathbb{R}$ describe the profits and costs of advertising, respectively. Similar first order PDE OC problems have also been considered in Barucci et al. 2001; Feichtinger et al. 2003, see also Grass et al. 2008, §8.3. In Faggian et al. 2013, some rigorous analysis (using results based on Barucci et al. 2001) is presented which inter alia yields the following:

[A] Assume that $\pi,\kappa{\in}L^2(\Omega)$, $v_0{\in}H^1(\Omega)$, $\kappa{>}0$, $\pi,v_0{\geq}0$, and take $\mathcal{W}=L^p_\rho([0,\infty),\mathbb{R}) = \{w:[0,\infty)\to\mathbb{R}_+, \int_0^\infty \mathrm{e}^{-\rho t}\|w(t)\|^p_{L^2}\,\mathrm{d}t\}$ as the set of admissible controls. Then (28) has a unique optimal advertising strategy $w^*=w^*(x)$, which in particular does not depend on t. The associated optimal solution $v^*:\Omega\times[0,\infty)$ is

$$v^*(x,t) = \mathrm{e}^{-\delta t}v_0(x-t)\chi_{[t,\omega]}(x) + \int_0^{\min t,x} \mathrm{e}^{-\delta s}\frac{\overline{\pi}(x-s)}{\kappa(x-s)}\,\mathrm{d}s, \quad (30)$$

where χ_I is the characteristic function of the interval I, i.e., $\chi_I(x)=1$ if $x\in I$, 0 else, and $\overline{\pi}\in H^1(\Omega)$ can be explicitly computed. In particular, for all $v_0\in H^1(\Omega)$, $v^*(\cdot,t)\to\hat{v}(\cdot)$ as $t\to\infty$, where $\hat{v}(x)=\int_0^x \mathrm{e}^{-\delta s}\frac{\overline{\pi}(x-s)}{\kappa(x-s)}\,\mathrm{d}s$.

Similar results can be obtained for related (linear–quadratic) models, which may also include boundary controls, see, e.g., Barucci et al. 2001; Faggian 2004. The proofs use some ideas from dynamic programming, and a posteriori yield a Pontryagin maximum principle. Additionally, Faggian et al. 2013 give and discuss some interesting explicit results for specific choices of π and κ.

We obtain the same results from directly applying the CS formalism as follows. The Lagrangian reads

$$L(v,\lambda,w) := \int_0^\infty \mathrm{e}^{-\rho t}\left\{\int_0^\omega \pi v - \frac{\kappa}{2}w^2 - \lambda(\partial_t v + \partial_x v + \delta v - w)\,\mathrm{d}x\right\}\mathrm{d}t, \quad (31)$$

and by integration by parts in t of $\int_0^\infty \mathrm{e}^{-\rho t}\int_\Omega \lambda\partial_t v\,\mathrm{d}x\,\mathrm{d}t$ (using the TC (19)), and integration by parts in x of $\int_\Omega \lambda\partial_x v\,\mathrm{d}x$, and taking first variations wrt λ and v we obtain

$$\partial_t v = -\partial_x v - \delta v + w, \quad v(x,0) = v_0(x), \quad v(0,t) = 0, \tag{32a}$$

$$\partial_t \lambda = -\partial_x \lambda + (\rho+\delta)\lambda - \pi, \quad \lambda(\omega,t) = 0, \tag{32b}$$

while $\delta_w L = 0$ yields $w = \lambda/\kappa$. Importantly, because J_c has no mixed term of the form vw, (32b) decouples from (32a) and can thus be discussed first. This is also at the core of the solution via dynamic programming. Here, (32b) has a unique steady solution $\hat{\lambda}(x)$, which can be computed to be $\kappa(x)w^*(x)$. Moreover, (32b) is ill-posed as an initial value problem because the BC $\lambda(\omega,t) = 0$ is on the 'wrong side' as the transport in (32b) is still to the right. Hence, $\hat{\lambda}(x)$ is *the only* feasible solution of (32b), and plugging $\hat{w} = \hat{\lambda}/\kappa$ back into (32a) we obtain (30). Moreover, concerning the (numerical) SPP in (26), the structure of (32a),(32b), i.e., the fact that (32b) is ill-posed and decoupled from (32a), yields that every pertubation of $\hat{\lambda}$ is in the unstable eigenspace of $\hat{u}$, and hence a priori $\lambda \equiv \hat{\lambda}$ for every canonical path.

All this is readily confirmed by applying the numerics from §3.2 to (32a),(32b). Additionally, for the numerics we can easily extend (28),(29) beyond the linear–quadratic case.

3.3.2 The spatial AK model

A problem which is particularly interesting to illustrate the role of the TC (19), is the 'spatial AK model' analyzed in Boucekkine et al. 2013 and Ballestra 2016. It reads

$$V(v_0) = \max_{c\in\mathcal{C}} J(v_0,c), \quad J(v_0,c) = \int_0^\infty \mathrm{e}^{-\rho t}\left(\int_\Omega \mathcal{U}(c(x,t))\,\mathrm{d}x\right)\mathrm{d}t, \quad \mathcal{U}(c) = \frac{c^{1-\sigma}}{1-\sigma}, \tag{33}$$

subject to the linear diffusion equation

$$\partial_t v = \partial_x^2 v + Av - c(t,x) \text{ in } \Omega = (0,2\pi), \quad v|_{t=0} = v_0, \tag{34}$$

with the periodic BC $v(0,t) = v(2\pi,t), \partial_x v(0,t) = \partial_x v(2\pi,t)$ (exactly the same results can be obtained for homogeneous Neumann BC $\partial_n v|_{\partial\Omega} = 0$ over general domains). Here, $v = v(x,t)$ is a distribution of capital, the control $c = c(x,t)$ is consumption, and $A, \rho > 0$ and $\sigma \in (0,1)$. In Boucekkine et al. 2013 the following result is shown via dynamic programming, and has been related to Pontryagin's Maximum Principle in Ballestra 2016:

[B] Assume that $A(1-\sigma) < \rho$, let $\eta = (\rho - A(1-\sigma))/(2\pi\sigma)$, $\beta = (A-\rho)/\sigma$ and $\overline{v}_0 = \int_0^{2\pi} v_0(x)\,\mathrm{d}x$. Then $c^* = c^*(t) = c_0\mathrm{e}^{\beta t}$ with $c_0 = \eta\overline{v}_0$ is the unique optimal control for (33).

In [B], the admissible controls fulfill $c, v \geq 0$ and a suitable limiting transversality condition, which fixes the constant c_0 in c^*, and which is discussed in detail and expressed in various ways in Boucekkine et al. 2013 and Ballestra 2016.

Here we want to illustrate that the CS formalism from §3.1 yields exactly the same result via the equivalent TC (19). The Lagrangian reads

$$L(v,\lambda,c)=\int_0^\infty \mathrm{e}^{-\rho t}\bigg(\int_\Omega \mathcal{U}(c)-\lambda(\partial_t v-\partial_x^2 v-Av+c)\,\mathrm{d}x\bigg)\,\mathrm{d}t,$$

and going through the integration by parts (using the pBC in x and the TC (19) in t) and taking first variations we obtain the CS

$$\partial_t v=\partial_x^2 v+Av-c,\quad c=\left(\frac{1}{\lambda}\right)^{1/\sigma},\quad v|_{t=0}=v_0, \tag{35a}$$

$$\partial_t\lambda=-\partial_x^2\lambda+(\rho-A)\lambda, \tag{35b}$$

with pBC for v and λ. Again, (35b) decouples, and has the general solution

$$\lambda(x,t)=\sum_{n\in\mathbb{N}_0}\mathrm{e}^{\mu_n t}(a_n\cos(nx)+b_n\sin(nx)),\ \mu_n=n^2+(\rho-A),\ a_n,b_n\in\mathbb{N},\ b_0=0, \tag{36}$$

but the non-negativity $\lambda>0$ (cause $c>0$) yields $a_n=b_n=0$ for all $n\in\mathbb{N}$. Thus, $\lambda(x,t)=\lambda(t)=\mathrm{e}^{(\rho-A)t}\lambda_0$ for some $\lambda_0>0$, and consequently

$$c(t)=\mathrm{e}^{(A-\rho)t/\sigma}c_0 \text{ with } c_0=(1/\lambda_0)^{1/\sigma}.$$

With $\mathrm{e}^{t\partial_x^2}$ the semigroup for the linear diffusion equation $\partial_t v=\partial_x^2 v$ on Ω, the solution $v(x,t)$ of (35a) then reads

$$v(x,t)=\mathrm{e}^{t(\partial_x^2+A)}v_0-c_0\int_0^t\mathrm{e}^{(t-s)A}\mathrm{e}^{\beta s}\,\mathrm{d}s=\mathrm{e}^{t(\partial_x^2+A)}v_0+c_0\mathrm{e}^{tA}\frac{1}{2\pi\eta}(\mathrm{e}^{\frac{1}{\sigma}(A(1-\sigma)-\rho)t}-1).$$

Since $\mathrm{e}^{t\partial_x^2}$ (with Neumann BC or periodic BC) conserves the average $\overline{v}=\int_\Omega v(x)\,\mathrm{d}x$, we obtain

$$\overline{v}(t)=\mathrm{e}^{tA}\bigg(\overline{v}_0+\frac{c_0}{\eta}\big(\mathrm{e}^{(A(1-\sigma)-\rho)t/\sigma}-1\big)\bigg).$$

For $A(1-\sigma)<\rho$ we have $\mathrm{e}^{(A(1-\sigma)-\rho)t/\sigma}\to 0$ for $t\to\infty$, and the TC

$$\begin{aligned}\lim_{t\to\infty}\mathrm{e}^{-\rho t}\int\lambda(t)v(x,t)\,\mathrm{d}x&=\lim_{t\to\infty}\mathrm{e}^{-\rho t}\lambda(t)\overline{v}(t)\\&=\lim_{t\to\infty}\mathrm{e}^{(A-\rho)t}\lambda_0\mathrm{e}^{(\rho-A)t}(\overline{v}_0+\frac{c_0}{\eta}(\mathrm{e}^{(A(1-\sigma)-\rho)t/\sigma}-1))\stackrel{!}{=}0\end{aligned}$$

uniquely fixes $c_0=\eta\overline{v}_0$ in dependence of the initial mass, illustrating the role of (19). In particular, if one (wrongly) chooses $c_0>c_0^*$, then $\overline{v}(t)\to-\infty$ as $t\to\infty$, clearly violating the assumption $v(x,t)\geq 0$ for all x,t, and $\lim_{t\to\infty}\mathrm{e}^{-\rho t}\lambda(t)\overline{v}(t)<0$. Conversely, if $c_0<c_0^*$ then $\lim_{t\to\infty}\mathrm{e}^{-\rho t}\lambda(t)\overline{v}(t)>0$, and consumption is smaller than optimal.

Note that $\overline{v}(t),c(t)\to\infty$ if $\rho<A$ (long sighted consumers) and $\overline{v}(t),c(t)\to 0$ if $\rho>A$ (short sighted consumers), and in these cases the method from §3.2 does not apply. In the special case $\rho=A$, for which $c^*(t)\equiv c_0=\eta\overline{v}_0$, we have (for fixed parameter values) a line $\{(\hat{v},\hat{\lambda}):\hat{v}>0,\hat{\lambda}=1/(\eta\hat{v})^\sigma\}$ of spatially constant CSSs, parametrized by the mass $\hat{v}$. These are 'weak' saddle–points in the sense that one eigenvalue always equals zero, and given a non-negative initial state $v_0=v_0(x)$ we obtain a unique CP to the CSS with $\hat{v}=\overline{v}_0$.

4 Results for the scalar fishery problems

We return to (5) and want to compute CSSs and CPs, starting with $f = f_{\text{lin}}$ and $f_{\log}$. While in general we need numerics already for CSSs, for the case $f = f_{\text{lin}}$ in (5) we can also compute the CSSs (semi–)analytically. This can be used to verify the numerics, and, via comparative statics, the modeling.

4.1 Linear growth and logistic growth

4.1.1 Semi-analytical CSSs for linear growth

For $f_{\text{lin}}(v) = \delta - \beta v$ the steady canonical system takes the form (without loss of generality choosing $D = 1$)

$$0 = v'' + \delta - \beta v, \qquad 0 = (\rho + \beta)\lambda - \lambda'', \tag{37a}$$

$$v'(0) = \gamma h, \quad v'(l) = 0, \qquad \lambda'(0) = -(p - \gamma\lambda)\partial_v h, \quad \lambda'(l) = 0. \tag{37b}$$

The ODEs in (37a) decouple, and the same holds true for the associated time dependent PDEs, which makes them superficially similar to the examples in §3.3) but the two problems are still coupled by the BC at x=0 in (37b). The general solution of (37a) is

$$v(x) = \delta/\beta + a_1 \mathrm{e}^{\sqrt{\beta}x} + b_1 \mathrm{e}^{-\sqrt{\beta}x}, \quad \lambda(x) = a_2 \mathrm{e}^{rx} + b_2 \mathrm{e}^{-rx}, \qquad r = \sqrt{\rho + \beta}, \tag{38}$$

and it remains to compute the constants a_1, a_2, b_1, b_2 from the BCs in (37b). From the Neumann BC at $x = l$ we get

$$b_1 = a_1 \mathrm{e}^{2\sqrt{\beta}l}, \quad b_2 = a_2 \mathrm{e}^{2rl}, \tag{39}$$

and thus end up with an algebraic system for a_1, a_2, namely

$$\sqrt{\beta} a_1 \big(\mathrm{e}^{2\sqrt{\beta}l} - 1\big) = \gamma k^{1-\alpha} v^{\alpha}, \qquad r a_2 \big(\mathrm{e}^{2rl-1}\big) = \alpha k^{1-\alpha} v^{\alpha-1}(p - \gamma\lambda), \tag{40}$$

together with $k = \left((1-\alpha)^2(p - \gamma\lambda)/c\right)^{1/\alpha}$, where it is understood that $\lambda = \lambda(0)$ and $v = v(0)$ are functions of a_1, a_2 via (38) and (39).

We now give a bio-economic discussion of the CSSs, aiming to illustrate general features. Letting

$$\Psi(x, a) := \frac{\mathrm{e}^{xa} + \mathrm{e}^{a(2l-x)}}{a(\mathrm{e}^{2la} - 1)},$$

the steady solutions of (37) can be implicitly written as

$$v(x) = \delta/\beta - \gamma h(v(0), k)\Psi(x, \beta), \qquad \lambda(x) = (p - \gamma\lambda(0))\, \partial_v h\,(v(0), k)\, \Psi(x, r),$$

with spatial dependence given by Ψ. The stock of the resource in the CSS equals its steady state value $v^* = \delta/\beta$ minus some decrement, which depends on x and the decay rate β, but does not (directly) depend on the discount rate ρ. Since Ψ is decreasing in x,

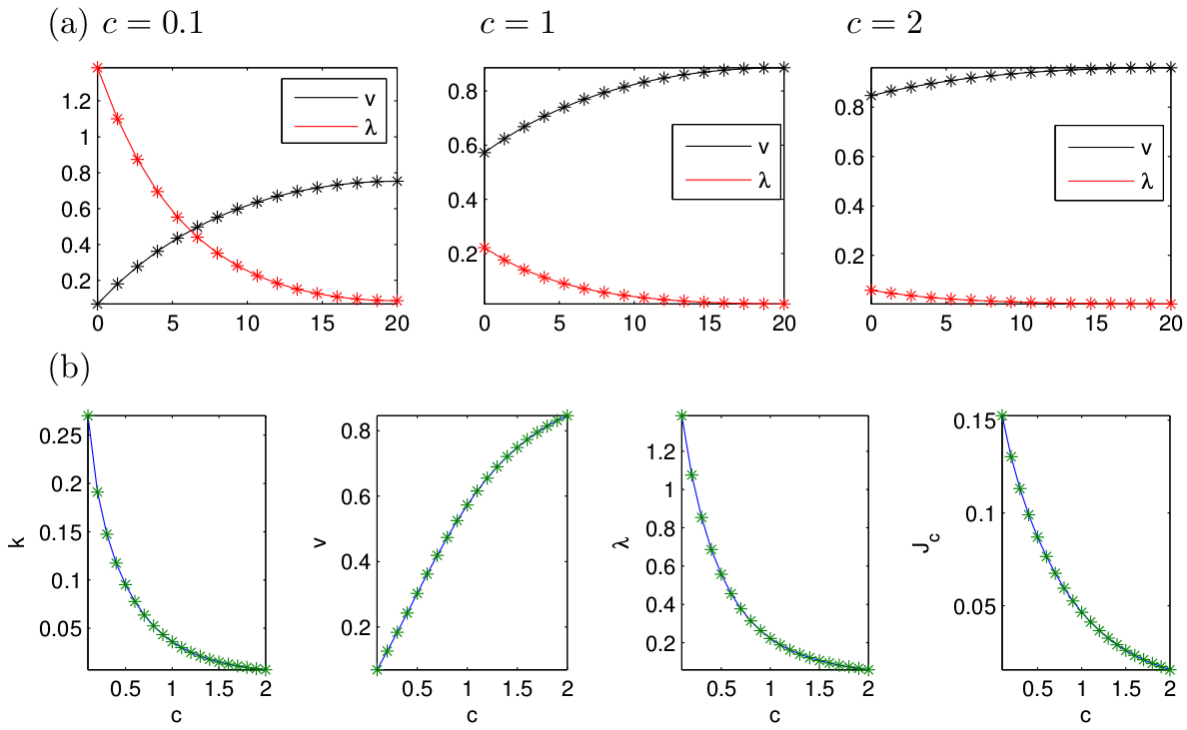

Figure 2: Some results for linear growth. In (a) we compare the solution (38) from (40) with parameters (41) (dots) with the direct numerical solution of (37) with `pde2path` (lines). Similarly, (b) compares the dependence of k, v, λ and J_c on c, computed via the two approaches.

the stock is higher and the shadow price is lower at more distant locations. Both results mirror the fact that a take out of fish exclusively takes place at the boundary $x = 0$. Due to the diffusion of fish, its removal at $x = 0$ is compensated by gradual replenishment, but since this process takes time the value of fish is lower at more distant locations.

System (40) cannot easily be solved algebraically for $a_{1,2}$, i. e., for $v(0), \lambda(0)$ and k, but it can immediately and conveniently be solved numerically in `Matlab` or similar systems. As an example, we choose the parameter specification

$$(\rho, \alpha, p, \gamma, \beta, \delta, l) = (0.02, 0.3, 1, 0.5, 0.01, 0.01, 20), \tag{41}$$

and let c vary between 0.1 and 2. For $c = 0.1, 1, 2$ we then obtain the unique solutions $(a_1, a_2) = (-0.167, 0.0014)$, $(a_1, a_2) = (-0.0077, 0.00022)$, and $(a_1, a_2) = (-0.0027, 0.00006)$, respectively. The associated solutions (38) are shown in Figure 2(a), and are indistinguishable from the direct numerical solution of (37) using `pde2path`.

Following §3.2, the next step would be to compute the time dependent CPs from an arbitray initial state v_0 (with $v_0(x) > 0$ for all x) to the (for fixed parameters) unique CSS which is always a saddle point, and the computation of their values. However, it turns out that the case $f = f_{\log}$ is quite similar to $f = f_{\text{lin}}$, and thus here we skip the presentation of CPs for $f = f_{\text{lin}}$ as we present CPs for $f = f_{\log}$ in §4.1.3.

4.1.2 Comparative statics

Figure 2(b) illustrates the dependence of the economically interesting quantities k, h, J_c and of $v(0), \lambda(0)$ on the effort cost c. Their qualitative behavior can also be obtained analytically, which in economics is called comparative statics. From (21e) and (40) we obtain $v = v(0)$, $\lambda = \lambda(0)$ and k as implicit functions of the cost parameter c. Using the shorthand $\Psi(a) = \Psi(0, a)$ we have

$$v = \frac{\delta}{\beta} - \gamma h\,(v,k)\,\Psi(\sqrt{\beta}),\ \ \lambda = (p-\gamma\lambda)\,\partial_v h\,(v,k)\,\Psi(r),\ \ c = (p-\gamma\lambda)\,(1-\alpha)\partial_k h\,(v,k)\,. \quad (42)$$

Implicitly differentiating (42) with respect to c, using $h(v,k) = v^\alpha k^{1-\alpha}$ and solving for the desired derivatives yields

$$v'(c) = \frac{v\gamma k^{\alpha+1}\Psi\left(\sqrt{\beta}\right)\left(vk^\alpha + k\alpha\gamma v^\alpha\Psi(r)\right)}{(1-\alpha)\alpha(p-\gamma\lambda)\left(vk^\alpha + k\gamma v^\alpha\Psi(r)\right)\left(vk^\alpha + k\gamma v^\alpha\Psi\left(\sqrt{\beta}\right)\right)} > 0, \quad (43a)$$

$$k'(c) = -\frac{k^{\alpha+1}v^{-\alpha}\left(vk^\alpha + k\alpha\gamma v^\alpha\Psi(r)\right)\left(vk^\alpha + k\alpha\gamma v^\alpha\Psi\left(\sqrt{\beta}\right)\right)}{(1-\alpha)^2\alpha(p-\gamma\lambda)\left(vk^\alpha + k\gamma v^\alpha\Psi(r)\right)\left(vk^\alpha + k\gamma v^\alpha\Psi\left(\sqrt{\beta}\right)\right)} < 0, \quad (43b)$$

$$\lambda'(c) = -\frac{k^{\alpha+1}\Psi(r)}{(1-\alpha)\left(vk^\alpha + k\gamma v^\alpha\Psi(r)\right)} < 0, \quad (43c)$$

$$h'(c) = -\frac{v'(c)}{\gamma\Psi\left(\sqrt{\beta}\right)} < 0. \quad (43d)$$

An increase in c renders harvesting effort more and more unattractive: effort k is reduced implying a reduction in harvest h, and thus an increase in the stock v; in parallel, higher costs reduce the value of the stock λ. Correspondingly, the resulting profit falls with higher values of c. Since the comparative effects (43) are unambiguous, it is clear that our numerical results depicted in Figure 2(b) are not due to our parameter specification but illustrate general features of our model.

4.1.3 Logistic growth

Similarly to the case $f = f_{\text{lin}}$, for $f = f_{\log}$ we again have unique CSSs $(v(x), \lambda(x))$ which look qualitatively and even quantitatively similar to those for $f = f_{\text{lin}}$. The reason for this similarity is that $f(v) = v(\delta - \beta v)$ is positive in the relevant range $0 < v < v^* = \delta/\beta$ (see also our discussion of the phase plane in §2.2). Accordingly, the dependence on parameters such as c is also qualitatively similar for logistic growth and linear growth. Moreover, it turns out that the unique CSSs $\hat{u}$ for both models are globally stable OSSs, i.e., for any $v_0 \geq 0$ (pointwise, with $v_0(x) > 0$ at least one point) there is a CP connecting v_0 to $\hat{u}$. In Fig. 3 we show two CPs for $f = f_{\log}$. In panels (a,b) we choose $v_0 \equiv 1$ (full initial stock in the domain), and in (c,d) $v_0 \equiv 0.1$ (almost depleted stock). (a) and (c) show the control k and the current value J_c at the left boundary as a function of time, while (b,c) show the associated evolutions of v.[3] The results are as expected: starting at a high (low) v_0, the

[3] In these and similar plots to follow, "`l1/pt13`" denotes the target CSS, following the `pde2path` style `branch/pointnumber` for solution labeling. In the surface plots $(x,t) \mapsto v(x,t)$ we only use a reduction

fishing effort decreases (increases) monotonically to that of the CSS. The main benefit of such a numerical computation is to find the precise quantitative behavior of $t \mapsto k(t)$.

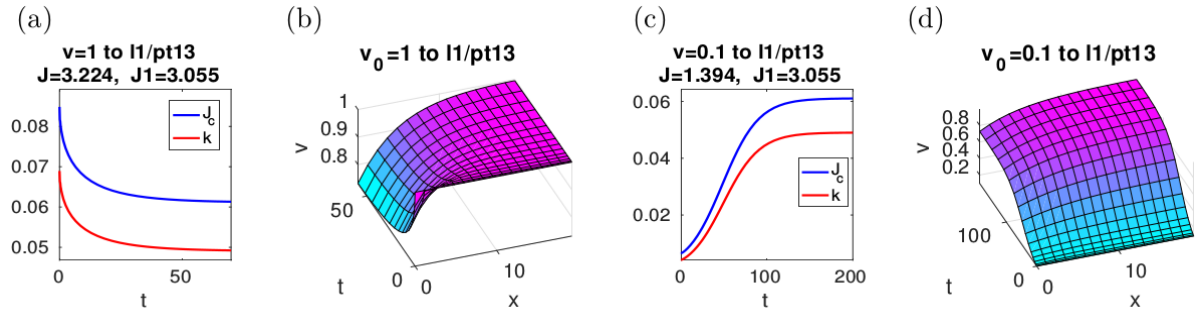

Figure 3: Example CPs connecting initial states v_0 to the unique globally stable CSS $\hat{u}$ for $f = f_{\log}$, $(\rho, \alpha, p, \gamma, \delta, \beta) = (0.02, 0.3, 1, 0.5, 0.01, 0.01)$, $c = 1$, and $v_0 \equiv 1$ in (a,b), and $v_0 \equiv 0.1$ in (c,d). (a,c) show k, J_c, while (b,d) illustrate the associated evolution of v. Here, $J = \int_0^\infty \mathrm{e}^{-\rho t} J_c(u(t))\,\mathrm{d}t$ and $J1 := \int_0^\infty \mathrm{e}^{-\rho t} J_c(\hat{u})\,\mathrm{d}t = \frac{1}{\rho} J_c(\hat{u})$ denote the values of the CP and of the target CSS, respectively.

4.2 Bistable growth

Compared with f_{lin} and $f_{\log}$, for $f = f_{\text{bi}}$ there are some important differences: depending on $v(l)$ (with $v'(l) = 0$) we may expect CSSs with v of the black, blue and magenta type indicated in Figure 1(d). We now fix $l = 10$, and, in contrast to Fig. 2 where we used the costs c as continuation parameter, we fix c and consider

$$(\alpha, p, \beta, \gamma, c) = (0.2, 8, 0.5, 1, 1), \tag{44}$$

as a base parameter set. We also first fix $\delta = 0.05$, and start with the discount rate ρ as our primary continuation parameter for the computation of (branches of) CSSs, because this turns out to be more convenient to obtain multiple CSSs. Subsequently we study the dependence of 'low stock CSSs' $\hat{u}(\cdot; \delta)$ on the 'regularization parameter' δ. We (numerically) find that $\lim_{\delta \to 0} \hat{u}(\cdot; \delta) = \hat{u}(\cdot, 0)$ where $\hat{u}(\cdot, 0)$ is a CSS of the formal limit system, and moreover, that the associated CPs also converge (uniformly in x and t) for $\delta \to 0$ to the limit CP. We also studied the dependence of CSSs and CPs on other parameters such as c as we did for $f = f_{\text{lin}}$ in Fig. 2. This dependence is as expected (similar to Fig. 2), and thus we refrain from presenting these results in detail, and only note that f_{bi} yields similar comparative statics results with respect to the parameters (α, p, γ, c) as f_{lin} and $f_{\log}$.

of the computational grid for plotting, i.e., typically every 3rd or 4th point in x and t directions. The computation of the CPs uses adaptive mesh-refinement in t, which usually occurs at the fast transitions at the start of the CPs.

Remark 4.1 In the derivation of (21) we assume the differentiability of h in v and k, and thus we need $v(0,t) > 0$ and $k(t) > 0$ for all $t \geq 0$. On the other hand, given (21e) we may eliminate k from (21a)–(21d) and find that $h(v,k) = v^\alpha k^{1-\alpha} = \widetilde{k}(\lambda)^{1-\alpha} v$ such that

$$\partial_v h = \widetilde{k}(\lambda)^{1-\alpha} \tag{45}$$

exists also for $v = 0$. This will now be relevant for $f = f_{\text{bi}}$ when we let the small regularization parameter $\delta > 0$ go to 0. We find a branch of CSSs $\hat{u}(\cdot;\delta)$ with monotonously increasing $0 < \hat{v}(\cdot;\delta) \approx \delta$, and monotonously decreasing $\hat{\lambda}(\cdot;\delta) > 0$. Moreover, for $\delta \to 0$ we find that $\hat{u}(\cdot;\delta) \to \hat{u}_0(\cdot)$, with $\hat{v}_0 \equiv 0$ and $\hat{\lambda}_0$ the solution of (21) obtained from setting $\delta = 0$ and using (45), and that, given some initial state v_0 (with low stocks), the CPs to $\hat{u}(\cdot,\delta)$ converge to the CP to $\hat{u}_0(\cdot)$ as well. This justifies to use the CS (21) with (45) also for $\delta = 0$, although a direct derivation of (21) for this case fails due to the non-differentiability of h at $(v,k) = (0,0)$.

4.2.1 The case $\delta > 0$

Figure 4 illustrates that for the choice (44) and $\delta = 0.05$ we have up to four CSSs for, e.g., $\rho \in (\rho_0, \rho_1)$, where the left and right folds of the black branch are at $\rho_0 \approx 0.051$ and $\rho_1 \approx 0.11$, respectively. The continuation of this branch starts in the upper left with a solution obtained from an initial guess of the form $v(x) = 0.8 + 0.1x/l$ and $\lambda(x) = 1$. The CSSs on the first part (till the fold) have defect $d = 0$, on the middle part we have $d = 1$, and after the second fold $d = 0$ again. Here the 1st (2nd and 3rd) parts corresponds to solutions of 'black' ('blue') type in Fig. 1(d). Additionally we have the magenta branch obtained from an initial guess of the form $v(x) = \delta/2, \lambda(x) = 1$, with $d = 0$ throughout. The example solution plots in (b) show four CSSs at $\rho = 0.06$ from (a). If we continue an 'upper solution' such as `b1/pt14` in the costs c, then we obtain a very similar behavior as in Fig. 2 for $f = f_{\text{lin}}$ and for $f = f_{\log}$. Clearly, this can be expected from the phase portrait in Fig. 1(c), as northwest of and close to the fixed point $(v, v') = (1, 0)$ all three phase portraits are similar. Continuation in c of solutions from the other branches, including the magenta branch, behave accordingly.

However, in contrast to the case of f_{lin} and $f_{\log}$, the upper solutions are *not* globally stable, i.e., they cannot be reached from arbitrary initial states v_0. For illustration we fix $\rho = 0.06$ and thus have `b1/pt14, b1/pt42` and `b2/pt14` (magenta CSS) as possible target CSSs, while `b1/pt26` cannot be a target CSS as it has defect $d = 1 > 0$. It then depends on the initial state v_0, which CSS can be reached by a CP starting in v_0, and which of these CPs is optimal. In Fig. 5(a,b) we start with v_0 from the defective CSS `b1/pt26`. From this v_0 we can reach both, `b1/pt14`, and `b1/pt42`, and both are locally stable OSSs. To reach `b1/pt14` from v_0, we need to temporarily decrease k to almost 0, while k is almost constant on the CP to `b1/pt42`. Therefore, even though the CSS `b1/pt42` has a significantly lower value ($J_1 = 7.11$) than the CSS `b1/pt14` ($J_1 = 15.04$),

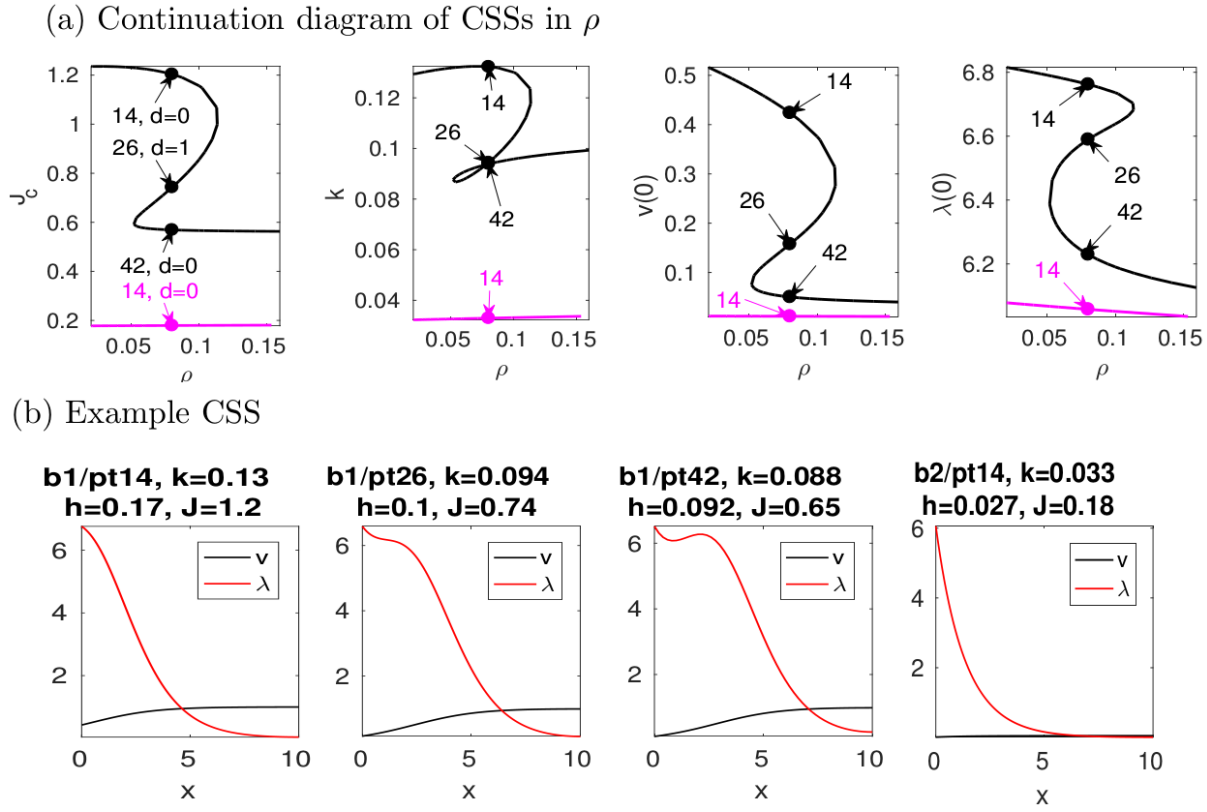

Figure 4: CSSs for $f = f_{\text{bi}}$, parameters from (44), $\delta = 0.05$. (a) Continuation in ρ of two branches of CSSs, leading to multiple CSSs (at fixed parameter values). $d = 0$ (saddle points) and $d = 1$ refers to the defects of the CSS on the respective (sections of the) branches. (b) Example CSS from the points marked in (a), b1=black branch, b2=magenta branch, cf. [3] for the naming convention.

in this case it is preferable to control the system towards `b1/pt42`: For the CP to `b1/pt42` we obtain $J \approx 9.76$, while the CP to `b1/pt14` only yields $J \approx 8.83$. A CP to the low stock CSS `b2/pt14` does not exist.

In Fig. 5(c) we give an illustration of the possible 'waiting time' phenomenon associated with CPs going to a CSS with a large stock, when the initial stock at $x = 0$ is low while there is sufficient stock in the rest of the domain. Here we choose $v_0 = \max(0.2 + x/10, 1)$. A CP to `b1/pt14` exists and has $k(t) \approx 0$ until at $t \approx 8$ the diffusion has led to a sufficient growth of the stock at $x = 0$. Nevertheless, for this v_0 again the path to `b1/pt42` (not shown) is dominant as it yields $J \approx 8.95$.

Due to the maximum principle for diffusion and the fact that $f(v) < 0$ for $0 \le \delta < v < \beta$, for all v_0 with $0 < v_0(x) \le \beta$ for all x the stock cannot increase beyond β at any point. Consequently, the only target CSSs that can be reached are those from the magenta branch. In Fig. 5(d) we consider $v_0 \equiv 0.4$ as an example. Here, the optimal strategy is to start with a large harvesting effort k which then monotonously decreases to that of the CSS. More generally, motivated by the bistability of f_{bi} we introduce the set of 'sub-threshold' initial states, which means that *only* a CP towards a low–stock CSS from

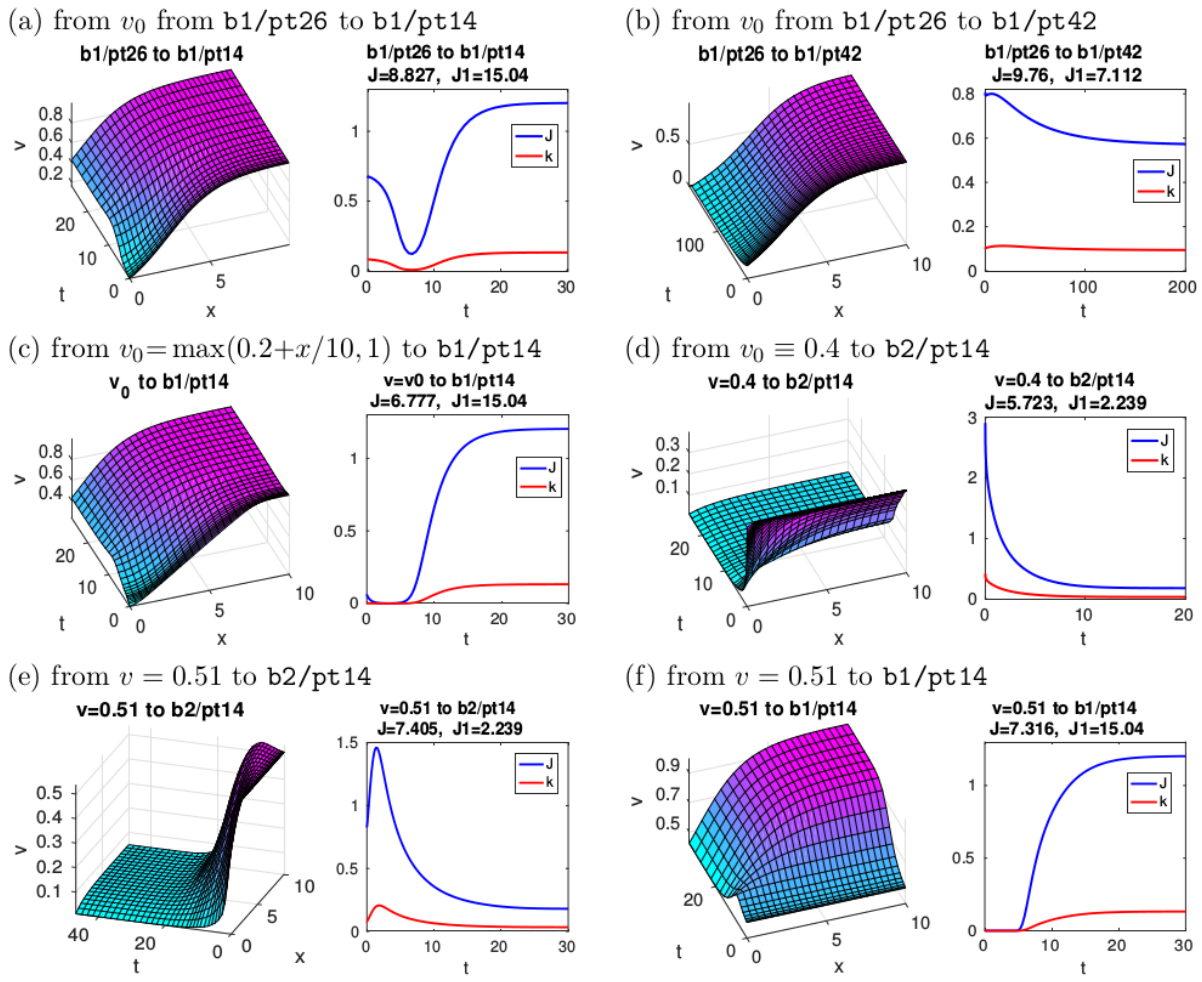

Figure 5: Example CPs for $f{=}f_{\rm bi}$, parameters from (44), $\delta{=}0.05$. In the time-series plots, J and $J1$ give the values of the CP and the target CSS, respectively. In (a) and (b) we use the same initial state v_0 from the defective CSS `b1/pt26`, but connect to the two different saddle-point CSSs on the black branch; The CP in (b) gives a somewhat higher J, although the target in (a) has a higher $J1$. (c) Example of a CP with 'waiting time' for the stock to first increase at $x{=}0$. (d) Example CP for the 'sub-threshold' initial state $v{\equiv}0.4{<}\beta{=}0.5$, connecting to the magenta CSS `b2/pt14`. (e,f) Two CPs for the constant 'intermediate' initial state $v \equiv 0.51$.

the magenta branch exists, and the set of 'super-threshold' initial states, for which *only* CPs towards the high–stock CSSs exist, where one could further distinguish between the analogs of `b1/pt14` and `b1/pt42`. Initial states for which CPs towards both, low–stock and high–stock CSSs exist are then called 'intermediate'. In Fig. 5(e,f) we consider such an intermediate case, namely $v_0{\equiv}0.51$. Here, CPs to `b2/pt14` and to `b1/p14` (but not to `b1/pt42`) exist. The resulting profit $J{\approx}7.405$ is (slightly) higher by going to the low-stock CSS (e) than by going to the high stock CSS (f) with $J{\approx}7.316$, as, interestingly, the latter is again associated with a waiting time (k almost 0), during which the stock increases uniformly.

A constant $v_0 > v_0^0 \approx 0.52$ turns out to be super–threshold. Of course, a precise characterization of the sub–threshold, super–threshold, and intermediate sets would be

tantamount to the computation of the 'basins of attraction' (Grass et al. 2008, p237ff) of the analogs of `b2/pt14`, and `b1/pt14` and `b1/pt42` at a given set of parameters, which is not feasible for the present infinite dimensional PDE constrained problem, or even for the high dimensional ODE problem obtained by spatial discretization. However, our simulations show that in the class of constant v_0 the super-threshold is only slightly larger than β, and that generally speaking the intermediate set is rather small.

The 'upper' CSSs (with large stocks at $x = 0$, e.g., `b1/pt14`) only exist up to $\rho_1 \approx 0.11$. For higher discount rates (corresponding to more myopic fishers), only the lower black and the magenta CSSs exist, but the (rough) characterization of sub–threshold, intermediate, and super–threshold initial states, and the associated CPs, are similar. Thus, so far this example illustrates the following:

1. To get an idea about possible optimal paths, it is crucial to first have a thorough understanding of the multiple CSSs.
2. Given an initial state v_0 for which CPs to different CSSs exist (intermediate case), we need to compare the values of the CPs (not just of the target CSSs) to decide which CP is optimal.
3. Constant v_0 only slightly larger than β are super–threshold. Further examples for super-threshold v_0 are v_0 from `b1/pt26` and v_0 from Fig. 5(c), where in both cases a CP to `b2/pt14` does not exist; roughly speaking, most v_0 with $v_0(x)$ small at small x but $v_0(x)$ large at more distant locations are super-threshold. This shows that the boundary control is rather weak in the following sense. For a distributed control (without control constraints) we would expect that a CP to a low stock CSS exists for all initial states v_0 (even though this CP might not be optimal). For the boundary harvesting, such a CP often does not exist; the bulk of fish is safe on the right, and is not sufficiently strongly 'pulled over' by diffusion, and is thus protected.

4.2.2 Low stocks and the limit $\delta \to 0$

The magenta branch from Fig. 4 exists for all (small) $\delta > 0$. Moreover, via (45) we may a posteriori use the CS (21) also for $\delta = 0$. Doing so, we can analytically compute the analog of the magenta branch for $\delta = 0$. We have $\hat{v} \equiv 0$, and the ODE for λ becomes

$$D\lambda'' = (\rho - f'(0))\lambda, \tag{46}$$

where $f'(0)|_{\delta=0} = -\beta$, with the general solution

$$\lambda(x) = c_1 \mathrm{e}^{\nu x} + c_2 \mathrm{e}^{-\nu x}, \quad c_1, c_2 \in \mathbb{R}, \quad \nu = \sqrt{(\rho+\beta)/D}. \tag{47}$$

The boundary condition $\lambda'(l) = 0$ yields $c_2 = \mathrm{e}^{2\nu l} c_1$, and the boundary condition $-D\lambda'(0) = (p - \gamma\lambda(0))\widetilde{k}(\lambda)^{1-\alpha}$ (using (45)) then yields the algebraic equation

$$D\nu(\mathrm{e}^{2\nu l} - 1)c_1 = (p - \gamma c_1(1 + \mathrm{e}^{2\nu l}))\widetilde{k}(c_1(1 + \mathrm{e}^{2\nu l}))^{1-\alpha}, \tag{48}$$

which can easily be solved numerically for c_1 using a Newton method with initial guess $c_1 = 0$. The solution then can be cross-checked with the numerical `pde2path` solution of (21) for $\hat\lambda(x;0)$, and $\hat v(x;0) \equiv 0$, yielding a perfect match.

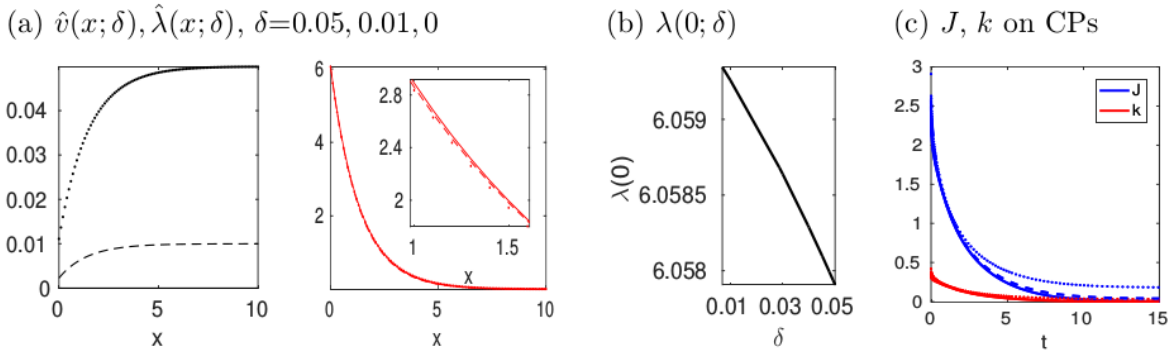

Figure 6: (a–b) Continuation of the CSS `b2/pt14` from Fig. 4 in δ, yielding a branch $\delta \mapsto \hat u(\cdot,\delta)$. (a) Spatial dependence of CSSs, δ=0.05 (dots), δ=0.01 (dashed) and δ=0 (full lines), with a zoom inset for $\hat\lambda$. (b) $\lambda(0;\delta)$ as a function of δ, with $\lim \lambda(0;\delta)$=$\lambda(0;0)$ with $\lambda(0;0)$ from (48). (c) J and k on CPs from $v_0 \equiv 0.4$ to the CSSs from (a), δ and linetypes as in (a).

Since the CS for $\delta = 0$ is only obtained formally, in Fig. 6 we illustrate the (numerical) convergence of the solutions for $\delta > 0$ to $\hat u(\cdot,0)$ as $\delta \to 0$. For this we continue the CSS from `b2/pt14` in δ, and in (a) we display $\hat v(\cdot;\delta)$ and $\hat\lambda(\cdot;\delta)$ for $\delta = 0.05, \delta = 0.01$, and $\delta = 0$. The plots of $\hat\lambda(\cdot,\delta)$ show that $\hat\lambda$ very weakly depends on δ, and the differences are only visible in the zoom. (b) illustrates the convergence of $\lambda(0;\delta)$, while all other quantities such as $v(0;\delta), k(\delta)$ converge to 0 for $\delta \to 0$. (c) illustrates the convergence of the CPs for fixed $v_0 \equiv 0.4$ (as in Fig. 4(a)) for $\delta \to 0$ to the CP $t \mapsto u^{(0)}(t)$ obtained for the formal limit CS ($\delta = 0$, full lines). Although we have no rigorous proof, this strongly suggests that $k^{(0)}(t)$ from $u^{(0)}(t)$ is the optimal control for $\delta = 0$ for such 'sub-threshold' initial states, for which, as expected, the harvesting effort decreases monotonically to 0. The CPs connecting to the upper black branch from Fig. 4 are hardly affected by changing δ, and thus we refrain from presenting these results.

5 Results for the predator-prey case

To apply the formalism from §3.1 to the vector valued problem (15), we introduce the co-states $\lambda_{1,2}$ and the Lagrangian

$$L(v,\lambda,k) = \int_0^\infty \mathrm{e}^{-\rho t}\left\{ J_c - \int_\Omega \langle \lambda, \partial_t v + G_1(v)\rangle \,\mathrm{d}x\right\}\mathrm{d}t,$$

where $\langle u, v\rangle = \sum_{i=1}^2 u_i v_i$ is the standard inner product in $\mathbb{R}^2$. Integration by parts in x and t with the transversality condition

$$\lim_{t\to\infty} \mathrm{e}^{-\rho t}\int_\Omega \langle \lambda(x,t)v(x,t)\rangle \,\mathrm{d}x = 0 \tag{49}$$

now yields

$$L(v,\lambda,k) = \int_\Omega \langle \lambda(0,\cdot), v(0,\cdot)\rangle \,\mathrm{d}x + \int_0^\infty \mathrm{e}^{-\rho t}\Big\{ [J_c - \langle \lambda, g\rangle - \langle D\partial_n\lambda, v\rangle]|_{x=0} - \langle D\partial_n\lambda, v\rangle\,|_{x=l} - \int_\Omega \langle \rho\lambda - \partial_t\lambda - D\Delta\lambda, v\rangle - \langle \lambda, f(v)\rangle \,\mathrm{d}x\Big\}\,\mathrm{d}t.$$

Then $\partial_v L = 0$ yields the evolution and the BCs of the co-states (combining with (10), to have it all together)

$$\left.\begin{aligned} &\partial_t v = D\Delta v + f(v),\\ &\partial_t \lambda = \rho\lambda - D\Delta\lambda - (\partial_v f(v))^T\lambda \end{aligned}\right\} \quad \text{in } \Omega = (0,l), \tag{50a}$$

$$\left.\begin{aligned} &D\partial_n v + g = 0,\\ &D\partial_n\lambda + \partial_v g(v)\lambda - \partial_v J_c = 0, \end{aligned}\right\} \quad \text{on the left boundary } x = 0, \tag{50b}$$

$$\left.\begin{aligned} &D\partial_n v = 0,\\ &D\partial_n\lambda = 0, \end{aligned}\right\} \quad \text{on the right boundary } x = l, \tag{50c}$$

and $\partial_k L = 0$ yields

$$k_j = \left(\frac{(1-\alpha_j)^2(p_j - \gamma_j\lambda_j)}{c_j}\right)^{1/\alpha_j} v_j, \quad j = 1,2. \tag{51}$$

As above, we first compute canonical steady states, i. e., we start with the stationary version $G(u) = 0$, $u = (v,\lambda)$ of (50), on $\Omega = (0,20)$. We choose the base parameter set

$$(\beta, d_1, d_2, \gamma_1, \gamma_2, \rho, \alpha_1, \alpha_2, p_1, p_2) = (0.6, 1, 10, 0.1, 0.1, 0.03, 0.4, 0.4, 20, 10), \tag{52}$$

and consider the costs (c_1, c_2) as our continuation parameters, starting with $c_1 = c_2 = 0.1$. By (52), we assume that the predators move faster than the prey, $d_2 = 10 > 1 = d_1$, and that the market price of the prey exceeds the price of the predator, $p_1 = 20 > 10 = p_2$, so that, disregarding the interaction of both species, the fisher is interested in catching the prey rather than the predator. Yet, in view of the interaction of the species, the fisher may consider catching the predator as well in order to "protect" the prey from the predator.

To find CSSs we use initial guesses of the form

$$v_1 = 1,\ v_2 = \delta(1-\beta),\ \lambda_1 = 50 + (1 - sx/l),\ \lambda_2 = 10 + (1 - sx/l), \tag{53}$$

with parameters $\delta \in (0,1)$ and s close to 1, and some variations of (53). But if an initial guess of this form yields convergence to a CSS, then (for the base parameters (52)) this convergence always leads to the same CSS. Note that a graphical phase plane analysis similar to §2.2 is no longer possible, and thus it is not clear how many CSSs may exist

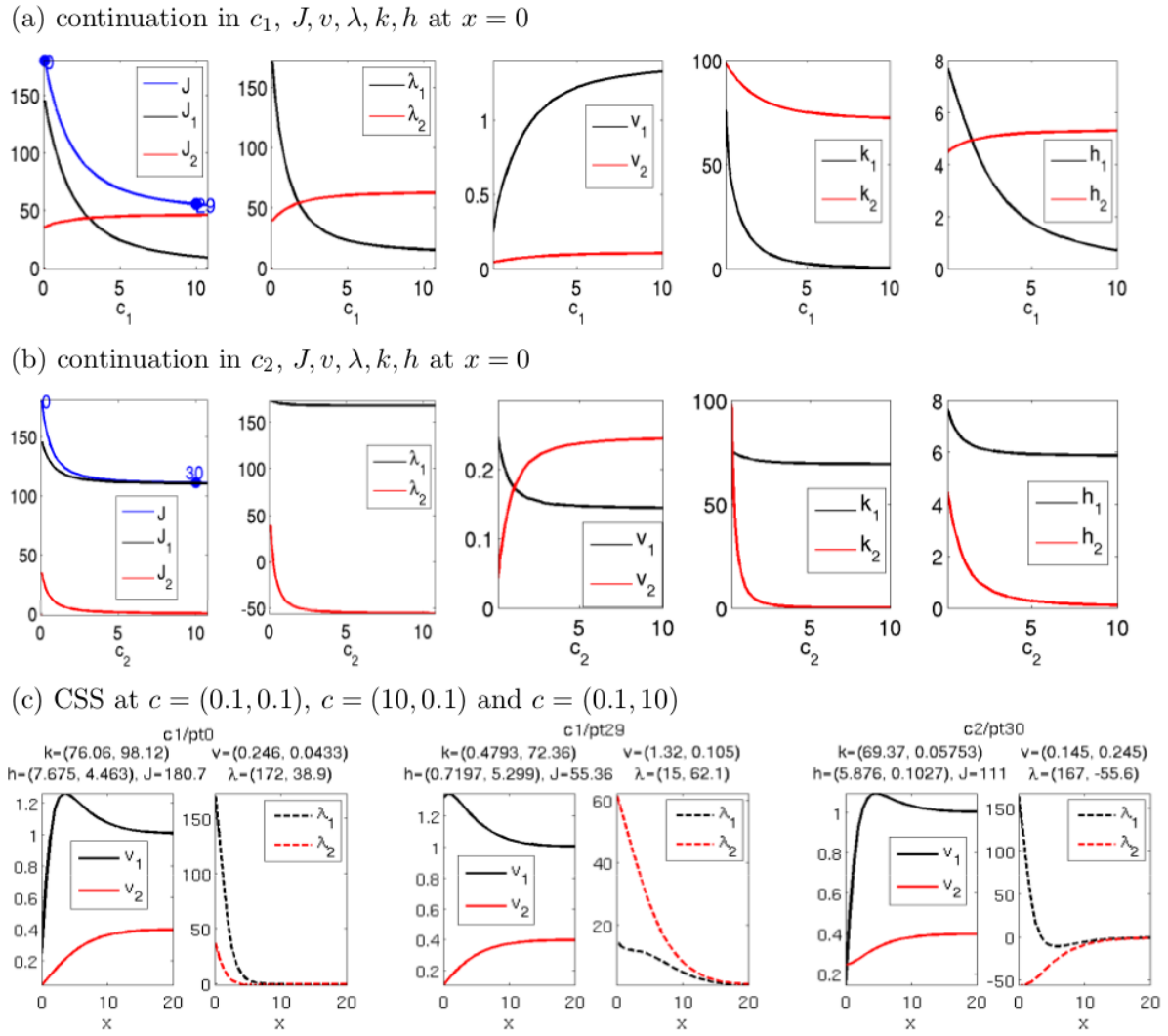

Figure 7: (a,b) continuation diagrams in c_1 (costs for prey fishing) and c_2 (costs for predator fishing); $J_j = p_j h_j - c_j k_j$, $J = J_1 + J_2$. For graphical reasons we restrict to $c_j \in [0.1, 10]$ (except for the plots of J) but all quantities continue as expected for $c_j \in [10, 20]$. (c) example CSS plots.

for (50). However, given that for $d_{1,2}$ sufficiently large and zero flux BCs V^* is the unique steady state of the Lotka–Volterra system (10), it appears reasonable to expect that for given parameters the system (50) has a unique CSS, as we assume rather large values for the diffusion parameters, $(d_1, d_2) = (1, 10)$, relative to the size of the domain.

Figure 7 depicts the CSSs and their dependence on the cost parameters (c_1, c_2).[4] (a) and (b) show relevant quantities at the left boundary as functions of c_1 and c_2, respectively, while (c) shows the spatial shape of the CSSs for selected values of (c_1, c_2). As expected, an increase in c_i $(i = 1, 2)$ leads to a reduction in effort k_i and the associated harvest h_i, and thus leads to a recovery of the stock v_i. In addition, an increase in c_i also imposes an indirect effect on v_{3-i} resulting from the interaction between both species. Consider

[4]We can extend our analysis in any parameter of the model, but as explained above we confine ourselves to an analysis of the economically most immediate parameters c_1 and c_2.

an increase in the effort cost c_1. There is no direct effect of c_1 on the fishing effort k_2 as its cost as well as the market price p_2 are unaffected. However, since an increase in c_1 results in less fishing effort k_1 and thus in a higher stock v_1, the living conditions of the predator species improve. Accordingly, the stock v_2 tends to increase, but since v_2 and k_2 are complements in the fishing technology, effort k_2 can be reduced with the catch h_2 still going up. Naturally, with higher cost c_1 the value of the the prey λ_1 falls, but the indirect effect makes the value of the predator λ_2 go up. The direct and the indirect effect of an increase in c_1 are also reflected in the profit terms. As expected, J_1 is a decreasing function of c_1, but the induced interaction effects between both species make J_2 to increase with c_1. Since the direct effect dominates, total profit J falls with higher cost.

Due to the biologically asymmetric situation of both species, an increase in c_2 has somewhat different indirect effects. In this case, higher c_2 leads to a reduction in effort k_2 and thus to an increase in the stock v_2. But with an increase of the predators the prey become more threatened, rendering this population to decline, and thus the fishing effort k_1 is reduced. In this way, since the increase in c_2 acts as a protection of the predator against being fished, the growth of that population exerts a negative effect on the prospects of fishing for the fisher. Accordingly, with the predator population becoming sufficiently large, the value of a unit of this species becomes negative. This explains why λ_2 is decreasing in c_2 and why it becomes (quickly) negative as the stock v_2 rises.

The qualitative structure of the spatial distribution of both species (and of the associated shadow prices) is quite robust with respect to changes in the costs c_1, c_2. Inspecting Figures 7(c1), (c2) and (c3), we infer that by catching the predator species the fisher makes sure that its stock is kept low at the coast (left boundary) so as to safeguard the prey there. In fact, the stock of the prey reaches its maximum close to the coast, but harvesting at the coast causes the stock to decrease drastically there (unless c_1 is very high, see Figure 7(c2)). In any case, fish located close to the coast is more worthy than at more distant locations, where it is inaccessible for the fisher, i. e., λ_1 and λ_2 are both decreasing in x. There is one exception, though: when, as explained above, c_2 is sufficiently large, such that it is very expensive to catch the predator species, this stock may swell until it interferes with the prospects of the fisher to catch the prey. In this case, the value of the predator is negative, $\lambda_2 < 0$, and because the damage caused by the predator species is the larger the closer it gets to the shore, λ_2 has its minimum directly at the shore.

In Figure 8 we illustrate the transition dynamics from the unique steady state (11) (with no fishing) to the CSS. Setting $(c_1, c_2) = (0.1, 0.1)$ in Figure 8(a) and $(c_1, c_2) = (20, 0.1)$ in Figure 8(b), these figures can directly be compared with Figure 7(c1) and Figure 7(c2), respectively. When the fishing cost of both species are low, $(c_1, c_2) = (0.1, 0.1)$, the transition to the CSS is accomplished by extensive fishing of both species at an initial phase, with fishing intensities decreasing from high towards low values. Thus,

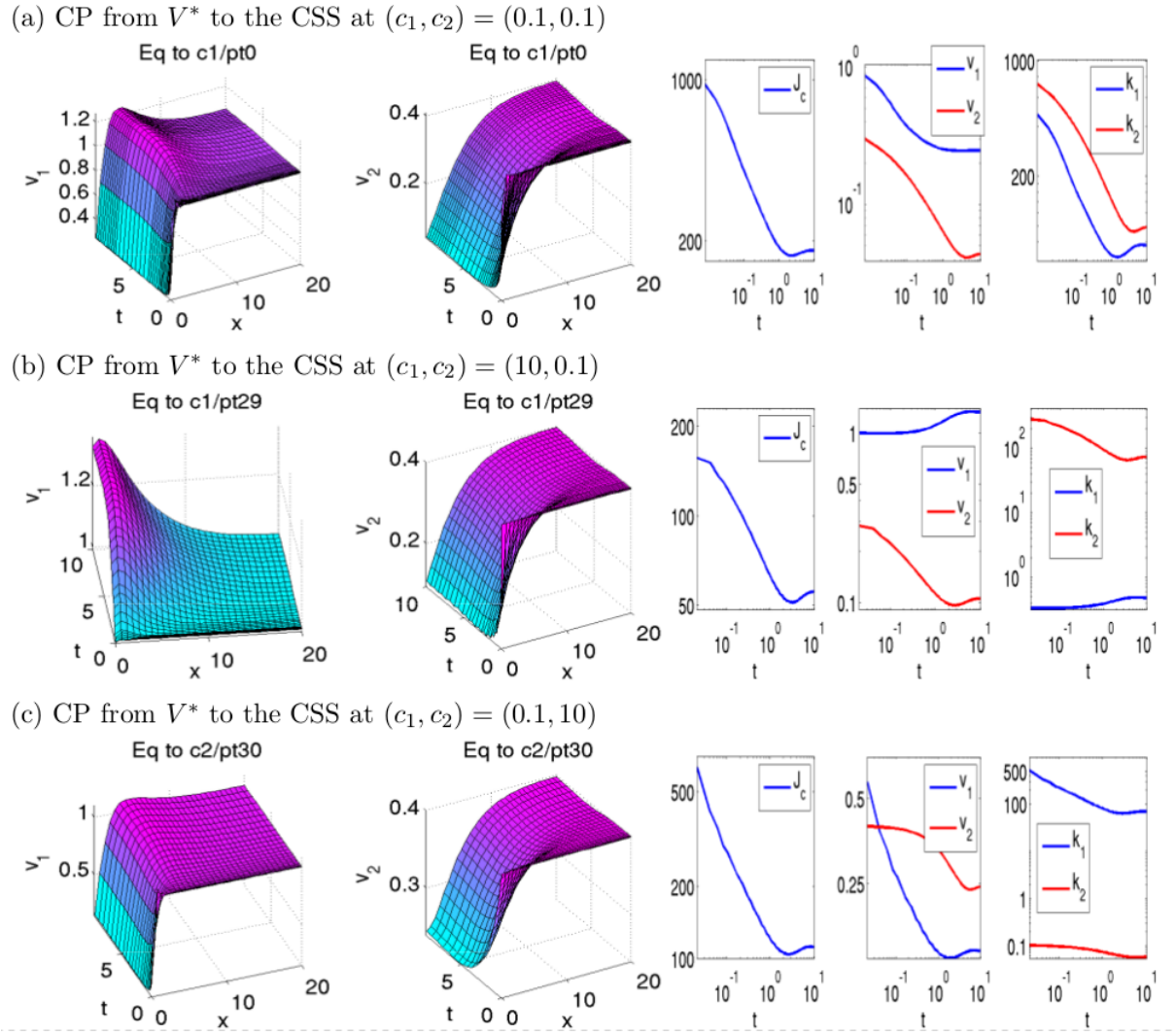

Figure 8: Canonical paths starting from the spatially homogeneous steady state V^* of (10).

there is a some initial overfishing, followed by a recovery phase during which the stocks of the CSS are reached from below, and during which the fisher increases the fishing intensity to that of the CSS.[5] If fishing the prey is very costly, $(c_1, c_2) = (10, 0.1)$, the CSS is characterized by a low effort level k_1 and hence by a high stock of the prey, cf. Figure 7(c2) and 8(b). Similarly, along the CP leading to the CSS the main harvest is on the predator, with fishing effort being reduced over time, leading to the gradual increase of the prey at the left boundary—and eventually on the complete domain. However, some harvesting activity on the prey still takes place. Finally, for $(c_1, c_2) = (0.1, 10)$, the roles are basically reversed, subject to the indirect effects resulting from the implicit protection of the predator species by a high effort cost c_2, as explained above.

[5]The initial transition is rather fast, and thus we use logarithmic scales in the time-series of the values at the left boundary.

6 Discussion and extensions

To the best of our knowledge, in resource economics this is the first detailed numerical (and in §4.1.1 semi-analytical) analysis of infinite time horizon optimal control problems with PDE constraints and a boundary control, beyond linear-quadratic models as reviewed in §3.3. We have set up one-species and two-species fishery models and characterized their canonical steady states (CSSs), which turned out to be unique globally stable optimal steady states (OSSs), except for the bistable case in the one–species model, for which multiple locally stable OSSs exist. Moreover, while previous studies in marine economics focus on the CSSs, we also compute the time-dependent canonical paths (CPs) connecting initial states to OSSs; these describe the policies that achieve the OSS in the most profitable way.

However, since our derivation of the canonical systems is formal in the sense detailed in §3.3, the CSSs and CPs obtained must be checked a posteriori for plausibility, but with this caveat the method seems highly effective. For the given examples, all results appear natural and intuitive, and they are robust with respect to alternative parameter specifications. The optimal policy compromises between immediate and future yield, taking into account that a higher stock left may favor future growth of the resource, and the optimal harvesting may feature 'waiting times' allowing the stock to grow before fishing starts. For the bistable case we can identify sub–threshold and super–threshold initial stocks, for which only CPs to low–stock CSSs resp. high–stock CSSs exist. For initial states from an 'intermediate' set we can go to both types of CSSs, and to determine which CP is optimal we need to compute the CPs and their values. This intermediate set turns out to be rather small, while the set of super–threshold initial states is rather large. This illustrates some natural limits of boundary controls compared with distributed controls.

For the two-species Lotka–Volterra model, the asymmetric interaction between both species provides an additional incentive to catch the predator species in order to protect the prey for the purpose of own take out. This asymmetry between both species carries over to the spatial distribution of the biomass of both species and their respective shadow prices: while the shadow price of the prey is decreasing in the distance to the location of the fisher, the shadow price of the predator may be higher at more distant locations, and may increase as the harvesting cost of the prey goes up.

Keeping the above caveat about the formal derivations of the canonical systems in mind, our approach can be extended to more complex and realistic models. One obvious way would be to generalize the one-dimensional problems by, for instance, considering either spatially dependent coefficients (of the PDEs), or more intricate multi-species fishery models; in addition, we may consider advection to model the transport of fish by flow. A second class of generalizations would be to extend the spatial domain to two (or even

three) dimensions. The spatial domain could either take the form of depth dependence of fishing at a fixed position in a river with one horizontal dimension, of a lake, or of a marine reserve in the open sea. In all these cases we have a boundary control function defined on a given part of the boundary, rather than a scalar control.

Similar boundary control models occur in other bio-economic circumstances. For instance, the shallow lake optimal control model deals with the phosphorus contamination of a lake, with the phosphate load, for instance from fertilizers, as control. Naturally, there is diffusion of the phosphorus, and thus a spatially extended model with a distributed control is studied in Grass et al. 2017. However, more realistically the phosphate load should be taken as a boundary control. Finally, models as in §3.3.1, including boundary controls, appear in a variety of settings, see for instance Faggian 2004 and the references therein. It will be interesting to extend these by genuine nonlinear terms. Moreover, as x in §3.3.1 models the age of consumers, and hence we have a transport equation for the goodwill, one could additionally introduce a spatial coordinate y for the location of consumers, which may diffuse in space, leading to a mixed 2D problem.

Acknowledgements. We thank the participants of the 16th Journées Louis-André Gérard-Varet, Aix-en-Provence, 2017; the Research Seminar on Environment, Resource and Climate Economics, MCC Berlin, 2017; 6th World Congress of Environmental and Resource Economists (WCERE), Gothenburg, Sweden; 14th Viennese Conference on Optimal Control and Dynamic Games, TU Wien; the 6th International Workshop on Heterogeneous Dynamic Models of Economic and Population Systems, WU Vienna and, in particular, Vladimir Veliov and Charles Figuières for valuable comments and suggestions.

References

Aniţa, S. (2000). *Analysis and Control of Age-Dependent Population Dynamics*. Kluwer Academic Publishers, Dordrecht.

Aniţa, S., V. Arnăutu, and V. Capasso (2011). *An introduction to optimal control problems in life sciences and economics*. Birkhäuser/Springer, New York.

Baker, C. M., F. Diele, C. Marangi, A. Martiradonna, and S. Ragni (2018). "Optimal spatiotemporal effort allocation for invasive species removal incorporating a removal handling time and budget". *Nat. Resour. Model.* 31.3, p. 12190.

Ballestra, L. V. (2016). "The spatial AK model and the Pontryagin maximum principle". *J. Math. Econom.* 67, pp. 87–94.

Barucci, E. and F. Gozzi (2001). "Technology adpotion and accumulation in a vintage capital model". *J. of Economics* 74.1, pp. 1–38.

Behringer, S. and T. Upmann (2014). "Optimal Harvesting of a Spatial Renewable Resource." *Journal of Economic Dynamics and Control* 42, pp. 105–120.

Beyn, W., T. Pampel, and W. Semmler (2001). "Dynamic optimization and Skiba sets in economic examples". *Optimal Control Applications and Methods* 22.5–6, pp. 251–280.

Boucekkine, R., C. Camacho, and G. Fabbri (2013). "Spatial dynamics and convergence: the spatial AK model". *J. Econom. Theory* 148.6, pp. 2719–2736.

Brock, W. A. and A. Xepapadeas (2008). "Diffusion-induced Instability and Pattern Formation in Infinite Horizon Recursive Optimal Control". *Journal of Economic Dynamics and Control* 32.9, pp. 2745–2787.

— (2010). "Pattern Formation, Spatial Externalities and Regulation in Coupled Economic-ecological Systems". *Journal of Environmental Economics and Management* 59.2, pp. 149–164.

Casas, E., J.-P. Raymond, and H. Zidani (2000). "Pontryagin's principle for local solutions of control problems with mixed control-state constraints". *SIAM J. Control Optim.* 39.4, pp. 1182–1203.

Casas, E. and F. Tröltzsch (2015). "Second order optimality conditions and their role in PDE control". *Jahresber. Dtsch. Math.-Ver.* 117.1, pp. 3–44.

Casas, E., C. Ryll, and F. Tröltzsch (2018). "Optimal control of a class of reaction–diffusion systems". *Comput. Optim. Appl.* 70.3, pp. 677–707.

Clark, C. W. (2010). *Mathematical Bioeconomics*. eng. 3rd. New Jersey: John Wiley & Sons.

Conrad, J. M. (2010). *Resource Economics*. eng. 2nd. Cambridge: Cambridge University Press.

Conrad, J. M. and C. W. Clark (1987). *Natural Resource Economics: Notes and Problems*. Cambridge University Press.

Da Lara, M. and L. Doyen (2008). *Sustainable Managment of Natural Resources: Mathematical Models and Methods*. Springer.

Ding, W. and S. Lenhart (2009). "Optimal Harvesting of a Spatially Explicit Fishery Model". *Natural Resource Modeling* 22.2, pp. 173–211.

Faggian, S. (2004). "Boundary-control problems with convex cost and dynamic programming in infinite dimension. I. The maximum principle". *Differential Integral Equations* 17.9-10, pp. 1149–1174.

Faggian, S. and L. Grosset (2013). "Optimal advertising strategies with age-structured goodwill". *Math. Methods Oper. Res.* 78.2, pp. 259–284.

Feichtinger, G., T. G., and V. Veliov (2003). "Optimality conditions for age-structured control systems". *J. Math Anal Appl.* 288.1, pp. 47–68.

Fister, K. R. (1997). "Optimal Control of Harvesting in a Predator-Prey Parabolic System". *Houston Journal of Mathematics* 23.2, pp. 341–355.

— (2001). "Optimal Control of Harvesting Coupled with Boundary Control in a Predator-Prey System," *Applicable Analysis* 77.1–2, pp. 11–28.

Fister, K. R. and S. Lenhart (2006). "Optimal Harvesting in an Age-Structured Predator-Prey Model". *Applied Mathematics and Optimization* 54.1, pp. 1–15.

Fogarty, M. J. and S. A. Murawski (2004). "Do Marine Protected Areas Really Work?" *Oceanus Magazine* 43.2, pp. 1–3.

Grass, D., J. P. Caulkins, G. Feichtinger, G. Tragler, and D. A. Behrens (2008). *Optimal Control of Nonlinear Processes: With Applications in Drugs, Corruption, and Terror*. Springer.

Grass, D. and H. Uecker (2017). "Optimal Management and Spatial Patterns in a Distributed Shallow Lake Model". *Electronic Journal of Differential Equations* 1, pp. 1–21.

Hastings, A. (1978). "Global Stability in Lotka-Volterra Systems with Diffusion". *Journal of Mathematical Biology* 6.2, pp. 163–168.

Hinze, M., R. Pinnau, M. Ulbrich, and S. Ulbrich (2009). *Optimization with PDE constraints*. Vol. 23. Mathematical Modelling: Theory and Applications. Springer, New York.

Kellner, J. B., I. Tetreault, S. D. Gaines, and R. M. Nisbet (2007). "Fishing the Line near Marine Reserves in Single and Multispecies Fisheries". *Ecological Applications* 17.4, pp. 1039–1054.

Kelly Jr., M. R., Y. Xing, and S. Lenhart (2016). "Optimal Fish Harvesting for a Population Modeled by a Nonlinear Parabolic Partial Differential Equation". *Natural Resource Modeling* 29.1, pp. 36–70.

Kunkel, P. and O. von dem Hagen (2000). "Numerical Solution of Infinite–Horizon Optimal–Control Problems". *Computational Economics* 16, pp. 189–205.

Lenhart, S. and J. Workman (2007). *Optimal Control Applied to Biological Models*. Chapman Hall.

Lenhart, S., M. Liang, and V. Protopopescu (1999). "Optimal control of boundary habitat hostility for interacting species". *Math. Methods Appl. Sci.* 22.13, pp. 1061–1077.

Leung, A. W. (1995). "Optimal Harvesting-Coefficient Control of Steady-State Prey Predator Diffusive Volterra-Lotka Systems". *Applied Mathematics and Optimization* 31.2, pp. 219–241.

Li, X. J. and J. M. Yong (1995). *Optimal control theory for infinite-dimensional systems*. Birkhäuser Boston.

Lions, J.-L. (1971). *Optimal Control of Systems Governed by Partial differential Equations*. Vol. 170. Grundlehren der mathematischen Wissenschaften. Berlin: Springer.

McCauley, D. J. et al. (2016). "Ending Hide and Seek at Sea". *Science* 351.6278, pp. 1148–1150.

Neubert, M. G. (2003). "Marine Reserves and Optimal Harvesting". *Ecology Letters* 6.9, pp. 843–849.

Pontryagin, L. S., V. G. Boltyanskii, R. V. Gamkrelidze, and E. F. Mishchenko (1962). *The Mathematical Theory of Optimal Processes*. Wiley-Interscience.

Raymond, J. P. and H. Zidani (1999). "Pontryagin's Principle for Time-Optimal Problems". *Journal of Optimization Theory and Applications* 101.2, pp. 375–402.

Sanchirico, J. N. and J. E. Wilen (1999). "Bioeconomics of Spatial Exploitation in a Patchy Environment". *Journal of Environmental Economics and Management* 37.2, pp. 129–150.

Serovaiskii, S. Y. (2003). *Counterexamples in Optimal Control Theory*. De Gruyter.

Tauchnitz, N. (2015). "The Pontryagin maximum principle for nonlinear optimal control problems with infinite horizon". *J. Optim. Theory Appl.* 167.1, pp. 27–48.

Tröltzsch, F. (2010). *Optimal Control of Partial Differential Equations*. Vol. 112. Graduate Studies in Mathematics. American Mathematical Society, Providence, RI.

Uecker, H. (2016). “Optimal Control and Spatial Patterns in a Semi-Arid Grazing System”. *Natural Resource Modeling* 29.2, pp. 229–258.

— (2017). *Infinite time–horizon spatially distributed optimal control problems with pde2path — a tutorial*. Available at `http://www.staff.uni-oldenburg.de/hannes.uecker/pde2path/tutorials.html`.

— (2019). “Hopf bifurcation and time periodic orbits with pde2path – algorithms and applications”. *Comm. in Comp. Phys* 25.3, pp. 812–852.

Uecker, H., D. Wetzel, and J. D. M. Rademacher (2014). “pde2path — A Matlab Package for Continuation and Bifurcation in 2D Elliptic Systems”. *Numerical Mathematics: Theory, Methods and Applications* 7, pp. 58–106.

Wirl, F. (1996). “Pathways to Hopf bifurcation in dynamic, continuous time optimization problems”. *Journal of Optimization Theory and Applications* 91, pp. 299–320.

Xepapadeas, A. (2010). “The Spatial Dimension in Environmental and Resource Economics”. *Environment and Development Economics* 15.6, pp. 747–758.